Magnetohydrodynamic Stability of Two Streaming Superposed Viscoelastic Conducting Fluids

Mohamed Fahmy El-Sayed

Department of Mathematics and Computer Science, Faculty of Science, U. A. E. University, P. O. Box 17551, Al Ain, United Arab Emirates;
Department of Mathematics, Faculty of Education, Ain Shams University, Roxy, Cairo, Egypt

Reprint requests to Dr. M. F. E.-S.; Fax: (9713) 7.671.291; E-mail: M.Elsayed@uaeu.ac.ae

Z. Naturforsch. **56 a,** 416–424 (2001); received December 13, 2000

The stability of the plane interface separating two Oldroydian viscoelastic superposed moving fluids of uniform densities when immersed in a uniform horizontal magnetic field has been investigated. The stability analysis has been carried out, for mathematical simplicity, for two highly viscous fluids of equal kinematic viscosities. It is found that the potentially stable configuration remains stable if the fluids are at rest, while it becomes unstable if the fluids move. The stability criterion is found to be independent of the viscosity and viscoelasticity, and to be dependent on the orientation of the magnetic field and the magnitudes of the fluids and Alfvén velocities. It is also found that the potentially unstable configuration remains unstable in the absence of average fluid velocities, or in the presence of fluid velocities and absence of a magnetic field. The magnetic field is found to stabilize a certain wavenumbers range of the unstable configuration even in the presence of the effects of viscoelasticity. The behaviour of growth rates with respect to the stress relaxation time, strain retardation time, fluid and Alfvén velocity parameters is examined analytically, and the stability conditions are obtained and discussed. – Pacs: 47.20.-k; 47.50.+d; 47.65.+a.

Key words: Hydrodynamic Stability; Non-Newtonian Fluid Flows; Magnetohydrodynamics.

1. Introduction

The Kelvin-Helmholtz instability of the plane interface between two incompressible fluids of different densities, when the lighter fluid is accelerated with respect to the heavier one, has been discussed by Chandrasekhar [1]. The problem of instability of a plane interface forming a vortex sheet between two fluids has been analyzed by several authors, because of its relevance to astrophysical [2, 3], geophysical [4, 5], and laboratory situations [6 - 8]. Such situations arise when air is blown over Mercury, or when a highly ionized hot plasma is surrounded by a colder ionized gas. This situation arises when a meteorite enters the Earth's atmosphere. Investigations of such a system have been analyzed by Chang and Russel [9], Wilson and Chang [10], Kalra et al. [11], and Lister and Hosking [12]. The investigation of Kelvin-Helmholtz instability of the interface separating two viscous rotating and conducting fluids permeated by a uniform horizontal magnetic field in the presence of finite ion-Larmor radius effects has been analyzed by Mehta and Bhatia [13].

Many fluids of interest in industrial practice exhibit non-Newtonian fluid behaviour. Extensive research has been undertaken over the last three decades, which has largely focussed on engineering analysis, such as the design of heat exchangers for non-Newtonian fluids. The study of interfacial instabilities in multilayer flow of viscoelastic fluids has received significant attention in recent years [14]. Such non-Newtonian fluids are widespread both in natural and industrial applications [15], for example as volcanic lava, mud flows, polymeric solutions, polycrystal melts, fluid suspensions, oil, paints, etc. Aside from their technical significance, multilayer flows can be effectively used to investigate the effect of fluid elasticity on the stability of generic viscoelastic flows with interfaces. Moreover, this calss of flows is of greate importance in various polymer processing operations, such as multilayer extrusion and coating, where a wide range of desired properties can be achieved by constructing a layerwise composite structure of various polymers. The Rayleigh-Taylor instability of viscoelatic fluids has been studied by many authors, for example, Sharma [16] studied the stability of a layer of Oldroyd

0932–0784 / 01 / 0600–0416 $ 06.00

fluid (i. e. fluid obeying Oldroyd's constitutive equation) heated from below and subject to a magnetic field. Eltayeb [17] studied the convective instability in a rapidly rotating viscoelastic (Oldroydian) fluid. Sharma [18] also studied the thermal instability of a layer of Oldroyd fluid acted on by a uniform rotation, the rotation being found to have a destabilizing as well as a stabilizing effect under certain conditions, in contrast to Maxwell fluids where it always has a destabilizing effect. The instability of the plane interface separating two viscoelastic superposed fluids of uniform densities has been studied by the Sharmas [19], [20], in the presence and absence of a uniform magnetic field, respectively. For recent excellent papers about hydrodynamic stability see [21 - 25].

The phenomenon of interfacial instability in the multilayer flow of immiscible Newtonian and Polymeric fluids has been studied by a number of investigators. Most studied have been theoretical and have employed the method of linear stability analysis [26 - 28], with the exception of a few attempts at weakly nonlinear analysis [29, 30]. Since the asymptotic methods are applicable only in the limit of long-wave and shortwave disturbances, Lee and Finlayson [31] studied the linear stability of a plane Couette flow at low Reynolds number of a Maxwell fluid using the shooting method. Yiantsios and Higgins [32] used the compound matrix numerical method to study the stability of the two layer plane Poiseuille flow of Newtonian fluids to a disturbance of arbitrary wavelength. Su and Khmoami [33] also used spectral based (namely spectral-tau and pseudospectal) techniques to analyze the stability of a superposed plane Poiseuille flow of Newtonian and viscoelastic fluids by using a number of quasilinear constitutive equations, such as the upper convected Maxwell, Oldroyd-B, and modified Oldroyd-B models. More recently, Ray et al. [34] studied the hydromagnetic stability of plane Couette flow at small Reynolds number of a conducting Oldroyd fluid in the presence of a transverse magnetic field, using the spectral Tau method to solve the obtained Orr-Sommerfeld equation.

It may be of some interest in chemical insudtry to study the Kelvin-Helmholtz instability of a plane interface separating two incompressible superposed viscoelastic fluids of uniform densities. This aspect forms the subject matter of the present paper, which to the best of my knowledge has not been investigated yet, wherein we have carried out the stability analysis for two fluids of equal kinematic viscosities and different uniform densities. The present analysis could be relevant for the stability of some polymer solutions.

2. Perturbation Equations

Consider the motion of an incompressible, infinitely conducting, viscoelastic Oldroydian fluid moving with velocity $\boldsymbol{U}(U(z), 0, 0)$ in the presence of a uniform magnetic field $\boldsymbol{H}(H_x, H_y, 0)$. Let τ_{ij}, e_{ij}, μ, λ, and $\lambda_0 (< \lambda)$ denote, respectively the shear stress tensor, the rate of the strain tensor, the dynamic viscosity, the stress relaxation time, and the strain retardation time. Assume that the viscoelastic fluid is described by the following constitutive relations:

$$\tau_{ij} = T_{ij} - p\delta_{ij}, \tag{1}$$

$$\left[1 + \lambda \frac{\mathrm{d}}{\mathrm{d}t}\right] T_{ij} = 2\mu \left[1 + \lambda_0 \frac{\mathrm{d}}{\mathrm{d}t}\right] e_{ij}, \tag{2}$$

$$e_{ij} = \frac{1}{2}\left[\frac{\partial u_i}{\partial x_j} + \frac{\partial u_j}{\partial x_i}\right], \tag{3}$$

where p is the isotropic pressure, δ_{ij} the Kronecker delta, $\mathrm{d}/\mathrm{d}t = \partial/\partial t + U_j(\partial/\partial x_j)$ is the mobile operator, while u_j and x_j are the velocity and position vectors, respectively. relations of the type (1 - 3) were first studied by Oldroyd [35], who showed that many rheological equations of state, of general validity, reduce to (1 - 3) when linearized. If $\lambda_0 = 0$, the fluid is Maxwellian, while if $\lambda_0 \neq 0$, we shall refer to the fluid as Oldroydian. The case when $\lambda = \lambda_0 = 0$ corresponds to a Newtonian viscous fluid. Here p, μ, and ρ are functions of the vertical coordinate z only.

Let $\boldsymbol{q}(u, v, w)$, $\delta\rho$, δp, and $\boldsymbol{h}(h_x, h_y, h_z)$ denote the perturbations in velocity, density, pressure, and magnetic field respectively. Then the linearized perturbation equations relevant to the problem are

$$\left\{1 + \lambda \frac{\partial}{\partial t}\right\} \rho \left[\frac{\partial \boldsymbol{q}}{\partial t} + U\frac{\partial \boldsymbol{q}}{\partial x} + w\frac{\mathrm{d}\boldsymbol{U}}{\mathrm{d}z}\right] = \tag{4}$$

$$\left\{1 + \lambda \frac{\partial}{\partial t}\right\} \left[-\nabla\, \delta p + \boldsymbol{g}\delta\rho + \frac{\mu_e}{4\pi}(\nabla \times \boldsymbol{h}) \times \boldsymbol{H}\right]$$

$$+ \rho\nu \left\{1 + \lambda_0 \frac{\partial}{\partial t}\right\} \nabla^2 \boldsymbol{q} + \left\{1 + \lambda_0 \frac{\partial}{\partial t}\right\} \left\{\frac{\partial w}{\partial x^*} + \frac{\partial \boldsymbol{q}}{\partial z}\right\} \frac{\mathrm{d}\mu}{\mathrm{d}z},$$

$$\nabla \cdot \boldsymbol{q} = 0, \tag{5}$$

$$\nabla \cdot \boldsymbol{h} = 0, \tag{6}$$

$$\left\{\frac{\partial}{\partial t} + U\frac{\partial}{\partial x}\right\}\delta\rho = -w\mathrm{D}\,\rho, \tag{7}$$

$$\left\{\frac{\partial}{\partial t} + U\frac{\partial}{\partial x}\right\}\boldsymbol{h} = \nabla \times (\boldsymbol{q} \times \boldsymbol{H}). \tag{8}$$

Equation (5) ensures that the density of every particle remains unchanged as we follow it with its motion, $\nu(=\mu/\rho)$ denotes the kinematic viscosity of the fluid, $\boldsymbol{g}(0,0,-g)$ is the acceleration due to gravity, $x^* = (x, y, z)$, and $\mathrm{D} = \mathrm{d}/\mathrm{d}\,z$.

Analyzing the disturbances into normal modes, we assume that the perturbed quantities have a space (x, y, z), and time (t) dependence of the form

$$f(z)\exp(ik_x x + ik_y y + nt), \tag{9}$$

where k_x, k_y are the horizontal wavenumbers, $k^2 = k_x^2 + k_y^2$, n is the growth rate of the harmonic disturbance, and $f(z)$ is some function of z.

For perturbations of the form (9), (4 - 8) become

$$\rho\left[(n + ik_x U)u + w\mathrm{D}\,U\right] =$$

$$-ik_x\delta p + \frac{\mu_e H_y}{4\pi}(ik_y h_x - ik_x h_y) \tag{10}$$

$$+\left\{\frac{1+\lambda_0 n}{1+\lambda n}\right\}\left[\rho\nu(\mathrm{D}^2 - k^2)u + (ik_x w + \mathrm{D}\,u)\mathrm{D}\,\mu\right],$$

$$\rho(n + ik_x U)v =$$

$$-ik_y\delta p + \frac{\mu_e H_x}{4\pi}(ik_x h_y - ik_y h_x) \tag{11}$$

$$+\left\{\frac{1+\lambda_0 n}{1+\lambda n}\right\}\left[\rho\nu(\mathrm{D}^2 - k^2)v + (ik_y w + \mathrm{D}\,v)\mathrm{D}\,\mu\right],$$

$$\rho(n + ik_x U)w = -\mathrm{D}\,\delta p - g\delta\rho \tag{12}$$

$$+\frac{\mu_e H_x}{4\pi}(ik_x h_z - \mathrm{D}\,h_x) + \frac{\mu_e H_y}{4\pi}(ik_y h_z - \mathrm{D}\,h_y)$$

$$+\left\{\frac{1+\lambda_0 n}{1+\lambda n}\right\}\left[\rho\nu(\mathrm{D}^2 - k^2)w + 2(\mathrm{D}\,w)(\mathrm{D}\,\mu)\right],$$

$$ik_x u + ik_y v + \mathrm{D}\,w = 0, \tag{13}$$

$$ik_x h_x + ik_y h_y + \mathrm{D}\,h_z = 0, \tag{14}$$

$$(n + ik_x U)\delta\rho = -w\mathrm{D}\,\rho, \tag{15}$$

$$(n + ik_x U)\boldsymbol{h} = (ik_x H_x + ik_y H_y)\boldsymbol{q}. \tag{16}$$

Multiplying (10) and (11) by $-ik_x$ and $-ik_y$, respectively, adding and using (13 - 16) in it, and finally eliminating δp between the resulting equation and (12), we obtain the following equation in w:

$$\mathrm{D}\left\{\rho(n + ik_x U)\mathrm{D}\,w\right\} - k^2\rho(n + ik_x U)w$$

$$-ik_x\mathrm{D}\,(\rho w\mathrm{D}\,U) = -\frac{gk^2(D\rho)w}{(n + ik_x U)} \tag{17}$$

$$-\frac{\mu_e(k_x H_x + k_y H_y)^2}{4\pi}(\mathrm{D}^2 - k^2)\left(\frac{w}{n + ik_x U}\right)$$

$$+\left\{\frac{1+\lambda_0 n}{1+\lambda n}\right\}\left[\mathrm{D}\left\{\rho\nu(\mathrm{D}^2 - k^2)\mathrm{D}\,w\right\} - k^2\rho\nu(D^2 - k^2)w\right]$$

$$+\left\{\frac{1+\lambda_0 n}{1+\lambda n}\right\}\left[\mathrm{D}\left\{(\mathrm{D}\,\mu)(\mathrm{D}^2 + k^2)w\right\} - 2k^2(\mathrm{D}\,\mu)(\mathrm{D}\,w)\right].$$

In the absence of fluid velocity, i. e. when $U = 0$, (17) reduces to the same equation for the corresponding Rayleigh-Taylor instability case studied by Sharma [19], and his results are therefore recovered. It should be noted here that the dispersion relation (when $U = 0$) obtained by Sharma [19], due to an error in algebra, is incorrect, and that fortunately this error does not affect his stability conditions. The correct dispersion relation is obtained as a limiting case of our work, when the fluid velocities are absent and the stability conditions are obtained and discussed in detail.

3. Boundary Conditions and Solutions

We consider here the case when two superposed viscoelastic Oldroydian fluids of uniform densities $\rho_1$and ρ_1, uniform velocities U_1 and U_2, and uniform viscosities μ_1 and μ_2 are separated by a horizontal boundary $z = 0$, in the presence of a uniform horizontal magnetic field. The subscripts 1 and 2 distinguish the lower and upper fluid, respectively. Then in each region of constant ρ, constant U, and constant μ, (17) becomes

$$(\mathrm{D}^2 - k^2)(\mathrm{D}^2 - K_j^2)w_j = 0,\ j = 1, 2, \tag{18}$$

where

$$K_j^2 = \tag{19}$$

$$k^2 + \frac{n + ik_x U_j}{\nu_j}\left\{\frac{1+\lambda n}{1+\lambda_0 n}\right\}\left\{1 + \frac{\mu_e(k_x H_x + k_y H_y)^2}{4\pi\rho_j(n + ik_x U_j)^2}\right\}.$$

Since w_j must vanish both when $z \to -\infty$ (in the lower fluid), and $z \to \infty$ (in the upper fluid), the general solutions of (18) can be written as

$$w_1 = \left[A_1 \exp(kz) + B_1 \exp(K_1 z)\right](n + ik_x U_1), \quad z < 0, \tag{20}$$

$$w_2 = \left[A_2 \exp(-kz) + B_1 \exp(-K_2 z)\right](n + ik_x U_2), \quad z > 0, \tag{21}$$

where A_1, B_1, A_2, and B_2 are constants of integration. In writing the solutions (20) and (21), it is assumed that K_1 and K_2 are defined such that their real parts are positive. The solutions (20) and (21) must satisfy certain boundary conditions. The boundary conditions to be satisfied at the interface $z = 0$ are

$$\frac{w_1}{(n + ik_x U_1)} = \frac{w_2}{(n + ik_x U_2)}, \tag{22}$$

$$\frac{\mathrm{D}\, w_1}{(n + ik_x U_1)} = \frac{\mathrm{D}\, w_2}{(n + ik_x U_2)}, \tag{23}$$

$$\frac{\mu_1(\mathrm{D}^2 + k^2) w_1}{(n + ik_x U_1)} = \frac{\mu_2(\mathrm{D}^2 + k^2) w_2}{(n + ik_x U_2)}. \tag{24}$$

Integrating (17) across the interface, we obtain another boundary condition, i. e.

$$\Delta_0\left[\rho(n + ik_x U)\mathrm{D}\, w\right] + \frac{\mu_e(k_x H_x + k_y H_y)^2}{4\pi}\Delta_0 \cdot \left[\mathrm{D}\left(\frac{w}{n + ik_x U}\right)\right] - \left\{\frac{1 + \lambda_0 n}{1 + \lambda n}\right\}\Delta_0\left[\rho\nu(\mathrm{D}^2 - k^2)\mathrm{D}\, w\right] = -gk^2\Delta_0(\rho)\left(\frac{w}{n + ik_x U}\right)_0 - 2k^2\left\{\frac{1 + \lambda_0 n}{1 + \lambda n}\right\} \cdot \Delta_0\left[\rho\nu(n + ik_x U)\right]\left(\frac{\mathrm{D}\, w}{n + ik_x U}\right)_0, \text{ at } z = 0, \tag{25}$$

where $\Delta_0(f)$ is the jump that a quantity f experiences at $z = 0$, and $(w/(n + ik_x U))_0$ is the unique value this quantity has at $z = 0$.

Applying the boundary conditions (22 - 25) to the solutions (20) and (21), we obtain

$$A_1 + B_1 = A_2 + B_2, \tag{26}$$

$$kA_1 + K_1 B_1 = -kA_2 - K_2 B_2, \tag{27}$$

$$\mu_1\left[2k^2 A_1 + (K_1^2 + k^2)B_1\right] = \mu_2\left[2k^2 A_2 + (K_2^2 + k^2)B_2\right], \tag{28}$$

and

$$\beta_1 A_1 + \gamma_1 B_1 + \beta_2 A_2 + \gamma_2 B_2 = 0 \tag{29}$$

where

$$\beta_j = -(1 + \lambda n) \cdot \left\{\alpha_j(n + ik_x U_j)^2 + (\boldsymbol{k} \cdot \boldsymbol{V}_\mathrm{A})^2 - \frac{gk}{2}(\alpha_2 - \alpha_1)\right\} \pm k^2(1 + \lambda_0 n)\left[\alpha_2\nu_2(n + ik_x U_2) - \alpha_1\nu_1(n + ik_x U_1)\right], \tag{30}$$

$$\gamma_j = \frac{gk}{2}(1 + \lambda n)(\alpha_2 - \alpha_1) \pm kK_j(1 + \lambda_0 n) \cdot \left[\alpha_2\nu_2(n + ik_x U_2) - \alpha_1\nu_1(n + ik_x U_1)\right], \tag{31}$$

and

$$\boldsymbol{V}_\mathrm{A} = \sqrt{\frac{\mu_e}{4\pi(\rho_1 + \rho_2)}}\,\boldsymbol{H},\ \alpha_j = \frac{\rho_j}{\rho_1 + \rho_2},\ j = 1, 2. \tag{32}$$

Here $\boldsymbol{k}$ is the wavenumber vector, and $\boldsymbol{V}_\mathrm{A}$ is the Alfvén velocity vector.

4. Stability Conditions and Discussion

Eliminating the constants A_1, B_1, A_2, and B_2 from (26 - 29), we obtain

$$\begin{vmatrix} 1 & 1 & -1 & -1 \\ k & K_1 & k & K_2 \\ 2k^2\mu_1 & \mu_1(K_1^2 + k^2) & -2k^2\mu_2 & -\mu_2(K_2^2 + k^2) \\ \beta_1 & \gamma_1 & \beta_2 & \gamma_2 \end{vmatrix} = 0. \tag{33}$$

This determinant can be reduced by subtracting the first column from the second, the third column from the fourth, and adding the first column to the third. Evaluating the resultant reduced determinant, we obtain the following characteristic equation:

$$2k\left[k(K_1 - k)(\alpha_1\nu_1 - \alpha_2\nu_2) - \alpha_1\nu_1(K_1^2 - k^2)\right] \times \left[(1 + \lambda n)\left\{\alpha_2(n + ik_x U_2)^2 + (\boldsymbol{k} \cdot \boldsymbol{V}_\mathrm{A})^2\right\} - k(K_2 - k) \times (1 + \lambda_0 n)\left\{\alpha_2\nu_2(n + ik_x U_2) - \alpha_1\nu_1(n + ik_x U_1)\right\}\right] - 2k\left[k(K_2 - k)(\alpha_1\nu_1 - \alpha_2\nu_2) + \alpha_2\nu_2(K_2^2 - k^2)\right] \times \left[(1 + \lambda n)\left\{\alpha_1(n + ik_x U_1)^2 + (\boldsymbol{k} \cdot \boldsymbol{V}_\mathrm{A})^2\right\} - k(K_1 - k)\right.$$

$$\times (1+\lambda_0 n)\{\alpha_2\nu_2(n+ik_xU_2)-\alpha_1\nu_1(n+ik_xU_1)\}]$$

$$-(1+\lambda n)[\alpha_1\nu_1(K_2-k)(K_1^2-k^2)+\alpha_2\nu_2(K_1-k)$$

$$\times (K_2^2-k^2)]\,[\alpha_1(n+ik_xU_1)^2+\alpha_2(n+ik_xU_2)^2$$

$$+2(\boldsymbol{k}\cdot\boldsymbol{V}_A)^2+gk(\alpha_1-\alpha_2)]=0. \tag{34}$$

The relation (34) is quite complicated, as the values of K_1 and K_2 involve square roots. We therefore make the assumption that the two fluids are highly viscous. Under this assumption, (19) yields

$$K_j=k\Big[1+\frac{n+ik_xU_j}{\nu_jk^2}\Big\{\frac{1+\lambda n}{1+\lambda_0 n}\Big\} \times\Big\{1+\frac{(\boldsymbol{k}\cdot\boldsymbol{V}_A)^2}{\alpha_j(n+ik_xU_j)^2}\Big\}\Big]^{1/2}, \tag{35}$$

so that

$$K_j=k+\frac{n+ik_xU_j}{2\nu_jk}\Big\{\frac{1+\lambda n}{1+\lambda_0 n}\Big\} \times\Big\{1+\frac{(\boldsymbol{k}\cdot\boldsymbol{V}_A)^2}{\alpha_j(n+ik_xU_j)^2}\Big\},\ j=1,2. \tag{36}$$

Substituting the values of (K_1-k) and (K_2-k) from (36) in (34), and putting $\nu_1=\nu_2=\nu$ (the case of equal kinematic viscosities for mathematical simplicity as in Chandrasekhar [1], but any of the essential features of the problem would not be obscured by this simplifying assumption), we obtain the following dispersion relation

$$\lambda^3n^5+\lambda^2n^4[(3+2\nu k^2\lambda_0)+2ik_x\lambda(\alpha_1U_1+\alpha_2U_2)]$$

$$+\lambda n^3[\lambda^2\{-k_x^2(\alpha_1U_1^2+\alpha_2U_2^2)+2(\boldsymbol{k}\cdot\boldsymbol{V}_A)^2$$

$$+gk(\alpha_1-\alpha_2)\}+\{3+2\nu k^2(\lambda+2\lambda_0)\}$$

$$+2ik_x\lambda(\alpha_1U_1+\alpha_2U_2)(3+\nu k^2\lambda_0)]$$

$$+n^2[3\lambda^2\{-k_x^2(\alpha_1U_1^2+\alpha_2U_2^2)+2(\boldsymbol{k}\cdot\boldsymbol{V}_A)^2$$

$$+gk(\alpha_1-\alpha_2)\}+\{1+2\nu k^2(2\lambda+\lambda_0)\}$$

$$+2ik_x\lambda(\alpha_1U_1+\alpha_2U_2)\{3+\nu k^2(\lambda+2\lambda_0)\}]$$

$$+n[3\lambda\{-k_x^2(\alpha_1U_1^2+\alpha_2U_2^2)+2(\boldsymbol{k}\cdot\boldsymbol{V}_A)^2$$

$$+gk(\alpha_1-\alpha_2)\}+2\nu k^2+2ik_x(\alpha_1U_1+\alpha_2U_2)$$

$$\times\{1+\nu k^2(2\lambda+\lambda_0)\}]+[\{-k_x^2(\alpha_1U_1^2+\alpha_2U_2^2)$$

$$+2(\boldsymbol{k}\cdot\boldsymbol{V}_A)^2+gk(\alpha_1-\alpha_2)\}$$

$$+2ik_xk^2\nu(\alpha_1U_1+\alpha_2U_2)]=0 \tag{37}$$

Note that in the absence of both fluid and Alfvén velocities, i.e. when $U_1=U_2=0$, and $\boldsymbol{V}_A=0$, the dispersion relation (37) reduces to the dispersion equation obtained earlier by Sharma and Sharma [20], and their results are therefore recovered. Now we need to consider both the stable and unstable cases of the considered system, in the presence of both fluid velocities and a uniform magnetic field.

(i) Stable Case $\alpha_1>\alpha_2$:

For the potentially stable arrangement $\alpha_1>\alpha_2$, and in the absence of fluid velocities, i.e. when $U_1=U_2=0$, we find by applying the Hurwitz criterion to (37), that (as all the coefficients in (37) are positive) all the roots of n are either real and negative, or there are complex roots with negative real parts. The system is therefore stable in each case. Thus in the absence of fluid velocities, the potentially stable configuration remains stable whether the fluid is viscoelastic or not. In the presence of fluid velocities there is one change of sign in (37), and so (37) has one positive root. The occurence of a positive root implies that the system is unstable. Thus the stable arrangement becomes unstable for the viscoelastic fluids described by Oldroyd's constitutive relation.

It can be seen from (37) that the system is stable in the corresponding Rayleigh-Taylor instability case ($U_1=U_2=0$) for all wavenumbers k even in the presence of effects of viscoelasticity. In the present Kelvin-Helmholtz instability case we find, by applying Hurwitz's criterion to (37), when $\alpha_1>\alpha_2$, that the system is stable for all wavenumbers which satisfy the inequality

$$k_x^2(\alpha_1U_1^2+\alpha_2U_2^2)<[2(\boldsymbol{k}\cdot\boldsymbol{V}_A)^2+gk(\alpha_1-\alpha_2)], \tag{38}$$

i.e. when

$$k<g(\alpha_1-\alpha_2)[(\alpha_1U_1^2+\alpha_2U_2^2)\cos^2\theta -2(V_1\cos\theta+V_2\sin\theta)^2]^{-1}, \tag{39}$$

where V_1 and V_2 are the Alfvén velocities in the x and y directions, and θ is the angle between $\boldsymbol{k}$ and $\boldsymbol{V}_A$; i. e. when $k_x = k\cos\theta$, $k_y = k\sin\theta$, θ being the orientation of the magnetic field.

(ii) Unstable Case $\alpha_1 < \alpha_2$*:*

For the potentially unstable configuration $\alpha_2 > \alpha_1$, and in the absence of fluid velocities, i. e. when $U_1 = U_2 = 0$, there is one change of sign in (37), and so (37) has one positive root. The occurence of a positive root implies that the system is unstable. Thus the unstable arrangement in this case remains unstable for the viscoelastic fluids described by Oldroyd's constitutive relation. It can be seen from (37), if the fluid velocities are included, that the system in this case is unstable in the hydrodynamic case $\boldsymbol{V}_A = 0$ for all wavenumbers k even in the presence of effects of viscoelasticity. In the present hydromagnetic case we find, by applying the Hurwitz criterion to (37), when $\alpha_2 > \alpha_1$, that the system is stable for all wavenumbers which satisfy the inequality

$$2(\boldsymbol{k}\cdot\boldsymbol{V}_A)^2 > \left[k_x^2(\alpha_1 U_1^2 + \alpha_2 U_2^2) + gk(\alpha_2 - \alpha_1)\right] \tag{40}$$

i. e. when

$$k > g(\alpha_2 - \alpha_1)\left[2(V_1\cos\theta + V_2\sin\theta)^2 - (\alpha_1 U_1^2 + \alpha_2 U_2^2)\cos^2\theta\right]^{-1}. \tag{41}$$

The stability criterion (41) is independent of the effects of viscosity and viscoelasticity. The magnetic field stabilizes a certain wavenumber range of the unstable configuration even in the presence of the effects of viscoelasticity. The critical wavenumber k^*, above which the system is stable, dependents on the magnitudes of the Alfvén velocities V_1, V_2, fluid velocities U_1, U_2, and fluid densities parameters α_1, α_2, as well as the orientation of the magnetic field θ. From the preceeding analysis we conclude that if we define the critical wavenumber k^* to be

$$k^* = g(\alpha_1 - \alpha_2)\left[(\alpha_1 U_1^2 + \alpha_2 U_2^2)\cos^2\theta - 2(V_1\cos\theta + V_2\sin\theta)^2\right]^{-1}, \tag{42}$$

then, for the stable configuration, the system will be stable in the wavenumber range $k < k^*$, while for the unstable configuration the system will be stable in the wavenumber range $k > k^*$, where k^* is given by (42). Otherwise, the system will be unstable.

On the other hand, the stability of the system can be checked using the asymptotic stability method elaborated by Zahreddine [36]. In this case (37) can be writen in the form

$$n^5 + a_1 n^4 + a_2 n^3 + a_3 n^2 + a_4 n + a_5 = 0, \tag{43}$$

where

$$a_1 = \lambda^{-1}\left[(3 + 2\nu k^2\lambda_0) + 2ik_x\lambda(\alpha_1 U_1 + \alpha_2 U_2)\right], \tag{44}$$

$$a_2 = \lambda^{-2}\left[\lambda^2\{-k_x^2(\alpha_1 U_1^2 + \alpha_2 U_2^2) + 2(\boldsymbol{k}\cdot\boldsymbol{V}_A)^2 + gk(\alpha_1 - \alpha_2)\} + \{3 + 2\nu k^2(\lambda + 2\lambda_0)\} + 2ik_x\lambda(\alpha_1 U_1 + \alpha_2 U_2)(3 + \nu k^2\lambda_0)\right], \tag{45}$$

$$a_3 = \lambda^{-3}\left[3\lambda^2\{-k_x^2(\alpha_1 U_1^2 + \alpha_2 U_2^2) + 2(\boldsymbol{k}\cdot\boldsymbol{V}_A)^2 + gk(\alpha_1 - \alpha_2)\} + \{1 + 2\nu k^2(2\lambda + \lambda_0)\} + 2ik_x\lambda(\alpha_1 U_1 + \alpha_2 U_2)\{3 + \nu k^2(\lambda + 2\lambda_0)\}\right], \tag{46}$$

$$a_4 = \lambda^{-3}\left[3\lambda\{-k_x^2(\alpha_1 U_1^2 + \alpha_2 U_2^2) + 2(\boldsymbol{k}\cdot\boldsymbol{V}_A)^2 + gk(\alpha_1 - \alpha_2)\} + 2\nu k^2 + 2ik_x(\alpha_1 U_1 + \alpha_2 U_2)\{1 + \nu k^2(2\lambda + \lambda_0)\}\right], \tag{47}$$

$$a_5 = \lambda^{-3}\left[\{-k_x^2(\alpha_1 U_1^2 + \alpha_2 U_2^2) + 2(\boldsymbol{k}\cdot\boldsymbol{V}_A)^2 + gk(\alpha_1 - \alpha_2)\} + 2ik_x k^2\nu(\alpha_1 U_1 + \alpha_2 U_2)\right]. \tag{48}$$

The polynomial (43) is asymptotically stable if and only if the following simultaneous conditions are strictly satisfied [36]:

$$\mathrm{Re}\, a_1 > 0, \text{ and } b_m > 0 \text{ for } m = 1, 2, 3, 4, \tag{49}$$

where

$$b_1 = (\mathrm{Re}\, a_1)^{-2}\left[(\mathrm{Re}\, a_1)\{(\mathrm{Re}\, a_1)(\mathrm{Re}\, a_2) + (\mathrm{Im} a_1)(\mathrm{Im}\, a_2) - (\mathrm{Re}\, a_3)\} - (\mathrm{Im}\, a_2)^2\right], \tag{50}$$

$$b_2 = b_1^{-2}\left[b_1\{b_1(\mathrm{Re}\, a_3) - ic_1(\mathrm{Im}\, a_2) - d_1(\mathrm{Re}\, a_1)\} + c_1^2(\mathrm{Re}\, a_1)\right], \tag{51}$$

$$b_3 = b_2^{-2}\left[b_2(b_2 d_1 - c_1 c_2 - b_1 d_2) + b_1 c_2^2\right], \tag{52}$$

$$b_4 = b_3^{-2}\left[b_3(b_3d_2 - c_2c_3) + b_2c_3^2\right], \tag{53}$$

and

$$c_1 = i(\mathrm{Re}\ a_1)^{-2}\left[(\mathrm{Re}\ a_1)\{(\mathrm{Re}\ a_1)(\mathrm{Im}\ a_3) - (\mathrm{Re}\ a_3)(\mathrm{Im}\ a_1) - (\mathrm{Im}\ a_4)\} + (\mathrm{Re}\ a_3)(\mathrm{Im}\ a_2)\right], \tag{54}$$

$$d_1 = (\mathrm{Re}\ a_1)^{-2}\left[(\mathrm{Re}\ a_1)\{(\mathrm{Re}\ a_1)(\mathrm{Re}\ a_4) + (\mathrm{Im}\ a_1)(\mathrm{Im}\ a_4) - (\mathrm{Re}\ a_5)\} - (\mathrm{Im}\ a_2)(\mathrm{Im}\ a_4)\right], \tag{55}$$

$$e_1 = i(\mathrm{Re}\ a_1)^{-2}\left[(\mathrm{Re}\ a_1)\{(\mathrm{Re}\ a_1)(\mathrm{Im}\ a_5) - (\mathrm{Re}\ a_5)(\mathrm{Im}\ a_1) + (\mathrm{Re}\ a_5)(\mathrm{Im}\ a_2)\right], \tag{56}$$

$$c_2 = b_1^{-2}\left[b_1\{ib_1(\mathrm{Im}\ a_4) - id_1(\mathrm{Im}\ a_2) - e_1(\mathrm{Re}\ a_1)\} + c_1d_1(\mathrm{Re}\ a_1)\right], \tag{57}$$

$$d_2 = b_1^{-2}\left[b_1\{b_1(\mathrm{Re}\ a_5) - ie_1(\mathrm{Im}\ a_2)\} + c_1e_1(\mathrm{Re}\ a_1)\right]. \tag{58}$$

$$c_3 = b_1^{-2}\left[b_2(b_2e_1 - c_1d_2) + b_1c_2d_2\right]. \tag{59}$$

The first condition in (49), $(\mathrm{Re}\ a_1) > 0$, gives $\lambda^{-1}(3 + 2\nu k^2\lambda_0) > 0$, which is automatically satisfied, while the second condition, $b_1 > 0$, leads to the condition

$$(\nu k^2\lambda^2\lambda_0)^{-1}\left[2\nu^2k^4\lambda_0(\lambda + 2\lambda_0) + \nu k^2(\lambda + 8\lambda_0) + 4\right] + \left\{-k_x^2(\alpha_1U_1^2 + \alpha_2U_2^2) + 2(\boldsymbol{k}\cdot\boldsymbol{V}_\mathrm{A})^2 + gk(\alpha_1 - \alpha_2)\right\} + 2k_x^2(\alpha_1U_1 + \alpha_2U_2)^2\left\{\frac{3 + \nu k^2\lambda_0}{3 + 2\nu k^2\lambda_0}\right\} > 0. \tag{60}$$

Three other conditions, corresponding to $b_2 > 0$, $b_3 > 0$, and $b_4 > 0$, respectively, can be obtained in a similar manner, and these conditions will not be given here because they are very lengthy. It follows that all these conditions can be simultaneously satisfied only if the condition

$$\left\{-k_x^2(\alpha_1U_1^2 + \alpha_2U_2^2) + 2(\boldsymbol{k}\cdot\boldsymbol{V}_\mathrm{A})^2 + gk(\alpha_1 - \alpha_2)\right\} > 0 \tag{61}$$

is satisfied, which coincides with the results given above; i. e. stability occurs for the wavenumber range $k < k^*$, when $\alpha_1 < \alpha_2$, and $k > k^*$ when $\alpha_1 > \alpha_2$. Otherwise, the system will be unstable.

We now wish to examine the behaviour of growth rates with respect to strain retardation time, Alfvén velocities, stress relaxation time, and fluid velocity parameters analytically. Let n_0 denotes the positive root, then from (37) we have

$$\begin{aligned}
&\lambda^3n_0^5 + \lambda^2n_0^4\left[(3 + 2\nu k^2\lambda_0) + 2ik_x\lambda(\alpha_1U_1 + \alpha_2U_2)\right] \\
&+ \lambda n_0^3\left[\lambda^2\{-k_x^2(\alpha_1U_1^2 + \alpha_2U_2^2) + 2(\boldsymbol{k}\cdot\boldsymbol{V}_\mathrm{A})^2 + gk(\alpha_1 - \alpha_2)\} + \{3 + 2\nu k^2(\lambda + 2\lambda_0)\} + 2ik_x\lambda(\alpha_1U_1 + \alpha_2U_2)(3 + \nu k^2\lambda_0)\right] \\
&+ n_0^2\left[3\lambda^2\{-k_x^2(\alpha_1U_1^2 + \alpha_2U_2^2) + 2(\boldsymbol{k}\cdot\boldsymbol{V}_\mathrm{A})^2 + gk(\alpha_1 - \alpha_2)\} + \{1 + 2\nu k^2(2\lambda + \lambda_0)\} + 2ik_x\lambda(\alpha_1U_1 + \alpha_2U_2)\{3 + \nu k^2(\lambda + 2\lambda_0)\}\right] \\
&+ n_0\left[3\lambda\{-k_x^2(\alpha_1U_1^2 + \alpha_2U_2^2) + 2(\boldsymbol{k}\cdot\boldsymbol{V}_\mathrm{A})^2 + gk(\alpha_1 - \alpha_2)\} + 2\nu k^2 + 2ik_x(\alpha_1U_1 + \alpha_2U_2) \times \{1 + \nu k^2(2\lambda + \lambda_0)\}\right] + \left[\{-k_x^2(\alpha_1U_1^2 + \alpha_2U_2^2) + 2(\boldsymbol{k}\cdot\boldsymbol{V}_\mathrm{A})^2 + gk(\alpha_1 - \alpha_2)\} + 2ik_xk^2\nu(\alpha_1U_1 + \alpha_2U_2)\right] = 0.
\end{aligned} \tag{62}$$

To study the behaviour of growth rates with respect to strain retardation time, Alfvén velocities, stress relaxation time, and fluid velocity parameters, we examine the nature of $\mathrm{d}n_0/\mathrm{d}\lambda_0$, $\mathrm{d}n_0/\mathrm{d}V_j$, $\mathrm{d}n_0/\mathrm{d}\lambda$, and $2d\,n_0/\mathrm{d}U_j$, $j = 1, 2$, respectively. It follows from (62) that

$$\frac{\mathrm{d}n_0}{\mathrm{d}\lambda_0} = -\frac{2\nu k^2n_0}{F}\{n_0(\lambda^2n_0^2 + 2\lambda\lambda_0n_0 + 1) + ik_x(\alpha_1U_1 + \alpha_2U_2)(\lambda n_0 + 1)^2\} \tag{63}$$

and

$$\frac{\mathrm{d}n_0}{\mathrm{d}V_j} = -\frac{4k_j}{F}(\boldsymbol{k}\cdot\boldsymbol{V}_\mathrm{A})(\lambda n_0 + 1)^3,\ j = 1, 2, \tag{64}$$

where

$$F = 5\lambda^3 n_0^4 + 4\lambda^2 n_0^3\left[(3+2\nu k^2\lambda_0) + 2ik_x\lambda(\alpha_1 U_1 + \alpha_2 U_2)\right] + 3\lambda n_0^2\left[\lambda^2\{-k_x^2(\alpha_1 U_1^2 + \alpha_2 U_2^2) + 2(\boldsymbol{k}\cdot\boldsymbol{V}_A)^2\right.$$

$$\left. + gk(\alpha_1-\alpha_2)\} + \{3+2\nu k^2(\lambda+2\lambda_0)\} + 2ik_x\lambda(\alpha_1 U_1+\alpha_2 U_2)(3+\nu k^2\lambda_0)\right] + 2n_0\left[3\lambda^2\{-k_x^2(\alpha_1 U_1^2+\alpha_2 U_2^2)\right.$$

$$\left. + 2(\boldsymbol{k}\cdot\boldsymbol{V}_A)^2 + gk(\alpha_1-\alpha_2)\} + \{1+2\nu k^2(2\lambda+\lambda_0)\} + 2ik_x\lambda(\alpha_1 U_1+\alpha_2 U_2)\{3+\nu k^2(\lambda+2\lambda_0)\}\right]$$

$$+ \left[3\lambda\{-k_x^2(\alpha_1 U_1^2+\alpha_2 U_2^2) + 2(\boldsymbol{k}\cdot\boldsymbol{V}_A)^2 + gk(\alpha_1-\alpha_2)\} + 2\nu k^2 + 2ik_x(\alpha_1 U_1+\alpha_2 U_2)\{1+\nu k^2(2\lambda+\lambda_0)\}\right]. \quad (65)$$

It is evident from (63) and (64) that both $\mathrm{d}n_0/\mathrm{d}\lambda_0$, and $\mathrm{d}n_0/\mathrm{d}V_j$ are positive or negative depending on whether the denominator F given in (65) is negative or positive, respectively. Thus, with increase in the strain retardation time, or in Alfvén velocities, the growth rate increases or decreases depending upon whether the denominator F is negative or positive, respectively. Therefore, the strain retardation time and the Alfvén velocities have boh stabilizing and destabilizing effects. Equation (62) yields also that

$$\frac{\mathrm{d}n_0}{\mathrm{d}\lambda} = -\frac{n_0}{F}\left\{3\lambda^2 n_0^4 + 2\lambda n_0^3\left[(3+2\nu k^2\lambda_0) + 3ik_x\lambda(\alpha_1 U_1+\alpha_2 U_2)\right] + n_0^2\left[3\lambda^2\left(-k_x^2(\alpha_1 U_1^2+\alpha_2 U_2^2)\right.\right.\right.$$

$$\left.\left.\left. + 2(\boldsymbol{k}\cdot\boldsymbol{V}_A)^2 + gk(\alpha_1-\alpha_2)\right) + 3 + 4\nu k^2(\lambda+\lambda_0) + 4ik_x\lambda(\alpha_1 U_1+\alpha_2 U_2)(3+\nu k^2\lambda_0)\right]\right.$$

$$+ n_0\left[6\lambda\left(-k_x^2(\alpha_1 U_1^2+\alpha_2 U_2^2) + 2(\boldsymbol{k}\cdot\boldsymbol{V}_A)^2 + gk(\alpha_1-\alpha_2)\right) + 4\nu k^2 + 2ik_x\lambda(\alpha_1 U_1+\alpha_2 U_2)\left(3+2\nu k^2(\lambda+\lambda_0)\right)\right]$$

$$\left. + \left[3\left(-k_x^2(\alpha_1 U_1^2+\alpha_2 U_2^2) + 2(\boldsymbol{k}\cdot\boldsymbol{V}_A)^2 + gk(\alpha_1-\alpha_2)\right) + 4ik_x k^2\nu(\alpha_1 U_1+\alpha_2 U_2)\right]\right\} \quad (66)$$

and

$$\frac{\mathrm{d}n_0}{\mathrm{d}U_j} = \frac{2k_x\alpha_j}{F}\left\{\lambda k_x U_j(\lambda n_0+1)^3 - i\left[\lambda^3 n_0^4 + \lambda^3 n_0^3(3+\nu k^2\lambda_0) + \lambda n_0^2\{3+\nu k^2(\lambda+2\lambda_0)\}\right.\right.$$

$$\left.\left. + n_0\{1+\nu k^2(2\lambda+\lambda_0)\} + \nu k^2\right]\right\},\ j = 1,2. \quad (67)$$

Following the arguments of the above paragraph, the stress relaxation time has a stabilizing effect depending upon whether the fractions in (66) are both positive or negative, respectively. Otherwise, the stress relaxation time has a destabilizing effect on the considered system. Note that if

$$k_x^2(\alpha_1 U_1^2+\alpha_2 U_2^2) < \left[2(\boldsymbol{k}\cdot\boldsymbol{V}_A)^2 - gk(\alpha_2-\alpha_1)\right], \quad (68)$$

where $\alpha_2 > \alpha_1$, is satisfied (or equivalently condition (40) holds), i.e. if the corresponding wavenumber range k satisfies the condition $k > k^*$, then $\mathrm{d}n_0/\mathrm{d}\lambda$, $\mathrm{d}n_0/\mathrm{d}\lambda_0$, and $\mathrm{d}n_0/\mathrm{d}V_j$ are negative Therefore, the stress relaxation time, the strain retardation time, and the Alfvén velocities, in this case, have stabilizing effects for the considered system; otherwise they will have destabilizing effects.

Also, from (67) it is clear that the growth rate (positive real part of n_0) increases on increasing the streaming velocities, showing thereby the destabilizing influence of the streaming fluid velocities U_1 and U_2. If the condition (68) is not satisfied, then all the physical quantity parameters will have stabilizing (for some wavenumbers) as well as destabilizing (for some other wavenumbers) effects on the stability of the considered configuration, as shown above.

In conclusion, this paper describes the effect of a uniform horizontal magnetic field on the viscous Kelvin-Helmholtz instability of the plane interface separating two superposed viscoelastic Oldroydian fluids, which is relevant for the stability of some polymer solutions. For the potentially stable arrangement ($\alpha_1 > \alpha_2$), we found that the system is stable in the absence of fluid velocities, and it is stable or unstable in the presence of fluid velocities under a certain condition for the velocities given by (38). The stability criterion in this case is found to be dependent only on the orientation of the magnetic field, and the magnitudes of both the fluid and Alfvén velocities.

For the potentially unstable configuration ($\alpha_1 < \alpha_2$), we found that the system is unstable in the cases of absence of fluid velocities or absence of a magnetic field, separately, while it is stable in the presence of fluid velocities under certain conditions for the Alfvén velocities given by (40). The critical wavenumber k^*, given by (42), under which or above which the system is stable, is obtained for the preceding two cases, respectively. The magnetic field is found to stabilize a certain wavenumber range of the unstable configuration, even in the presence of the effects of viscoelasticity. The stability of the system is studied also using the asymptotic stability method elaborated by Zahreddine [36], and the obtained stability condition confirms the previous results. Finally, for the behaviour of growth rates with respect to strain retardation time, Alfvén velocities, stress relaxation time, and fluid velocities, respectively, it is found that both the strain retardation time and the Alfvén velocities have stabilizing as well as destabilizing influences depending upon whether the quantity F given by (65) is positive or negative. It is found also that the relaxation time has a stabilizing as well as a destabilizing effects depending upon whether the fractions in (66) are simultaneously positive or negative, respectively, and stability holds only if condition (68) is satisfied, while the fluid velocities are found to have usually destabilizing effects. Therefore, all the physical quantities have stabilizing as well as destabilizing effects on the considered system under certain conditions.

Acknowledgements

The financial support of the Natural Sciences and Engineering Reaserch Council of the United Arab Emirates University is gratefully acknowlsdged. I would like also to thank Prof. F. Van Oystaeyen (Belgium) for his critical reading of the manuscript and his useful suggestions during his visit to the United Arab Emirates University in November, 1999.

[1] S. Chandrasekhar, Hydrodynamic and Hydromagnetic Stability, Dover Publications, New York 1981.
[2] S. P. Talwar and G. L. Kalra, Ann. Astrophys. **29**, 507 (1966).
[3] S. P. Talwar, Cosmic Electrodyn. **1**, 255 (1970).
[4] G. L. Kalra and S. P. Talwar, Monthly Notices Roy. Astron. Soc. **135**, 891 (1967).
[5] S. S. Rao, G. L. Kalra, and S. P. Talwar, J. Plasma Phys. **2**, 181 (1968).
[6] N. D'Angelo and S. Von Goelor, Phys. Fluids **9**, 309 (1966).
[7] J. R. Melcher, Phys. Fluids **9**, 1548 (1966).
[8] B. J. Daly, Phys. Fluids **10**, 297 (1967).
[9] I.-D. Chang and P. E. Russel, Phys. Fluids **8**, 1018 (1965).
[10] A. J. Willson and I.-D. Chang, Phys. Fluids **10**, 2285 (1967).
[11] G. L. Kalra, S. N. Katharia, R. J. Hosking, and G. G. Lister, J. Plasma Phys. **4**, 451 (1970).
[12] G. G. Lister and R. J. Hosking, J. Plasma Phys. **7**, 553 (1972).
[13] V. Mehta and P. K. Bhatia, Astrophys. Space Sci. **141**, 151 (1988).
[14] R. G. Larson, Rheol. Acta **31**, 213 (1992).
[15] Yu. A. Berezin, K. Hutter, and L. A. Spodareva, Physica D **139**, 319 (2000); Arch. Appl. Mech. **68**, 169 (1998).
[16] R. C. Sharma, Acta Phys. Hung. **38**, 293 (1975).
[17] I. A. Eltayeb, Zeit. Angew. Math. Mech. (ZAMM) **55**, 599 (1975).
[18] R. C. Sharma, Acta Phys. Hung. **40**, 11 (1976).
[19] R. C. Sharma, J. Math. and Phys. (India) **12**, 603 (1978).
[20] R. C. Sharma and K. C. Sharma, Acta Phys. Hung. **45**, 213 (1978).
[21] M. F. El-Sayed, Nuovo Cimento D **20**, 1645 (1998); Nuovo Cimento B **41**, 1305 (1999); Phys. Rev. E **60**, 7588 (1999); Physica A **291**, 211 (2001).
[22] M. F. El-Sayed, Z. Naturforsch. **55a**, 460 (2000); Czech. J. Phys. **50**, 607 (2000); Arch. Appl. Mech. (2001), in press.
[23] M. F. El-Sayed, Can. J. Phys. **75**, 499 (1997); Physica Scripta **55**, 350 (1997); **58**, 613 (1998); Physica A **255**, 1 (1998).
[24] M. F. El-Sayed and D. K. Callebaut, J. Colloid Interface Sci. **200**, 203 (1998); Physica Scripta **57**, 161 (1998); Z. Naturforsch. **53a**, 217 (1998); Physica A **269**, 235 (1999).
[25] H. K. Ganpule and B. Khomami, J. Non-Newtonian Fluid Mech. **80**, 217 (1999); **81**, 27 (1999).
[26] C.-S. Yih, J. Fluid Mech. **27**, 337 (1967).
[27] N. D. Walters, J. Non-Newtonian Fluid Mech. **12**, 85 (1983).
[28] B. Khomami, J. Non-Newtonian Fluid Mech. **37**, 19 (1990).
[29] R. Yuriko, Phys. Fluids. A **10**, 1666 (1989).
[30] A. P. Hopper and R. Grimshaw, Phys. Fluids **28**, 37 (1985).
[31] K. C. Lee and B. A. Finlayson, J. Non-Newtonian Fluid Mech. **21**, 65 (1986).
[32] S. G. Yiantsios and B. G. Higgins, Phys. Fluids **31**, 3225 (1988).
[33] Y. Y. Su and B. Khomami, Chem. Eng. Comm. **109**, 209 (1991); J. Comput. Phys. **100**, 297 (1992); J. Rheol. **36**, 2 (1992).
[34] R. N. Ray, A. Samad, and T. K. Chaudhury, Bull. Cal. Math. Soc. (India) **91**, 279 (1999).
[35] J. G. Oldroyd, Proc. Roy. Soc. London A **245**, 278 (1958).
[36] Z. Zahreddine, Indian J. Pure Appl. Math. **21**, 781 (1990).

Fluoroacetylenes and Deuterofluoroacetylenes, Synthesized in a Pulsed Discharge Nozzle; a Molecular Beam Fourier Transform Microwave Spectroscopy Study Combined with Quantum Chemical Calculations

D. H. Sutter and H. Dreizler

Institut für Physikalische Chemie der Christian-Albrechts-Universität zu Kiel, Olshausenstr. 40, D-24098 Kiel, Germany

Reprint requests to Prof. Dr. H. D; Fax: +49(0)431 8801416;
E-mail: Sutter@phc.uni-kiel.de, Dreizler@phc.uni-kiel.de

Z. Naturforsch. **56 a,** 425–439 (2001); received April 30, 2001

Dedicated to Prof. Dr. A. Guarnieri on occasion of his 70th birthday.

We report on the production of fluoroacetylene by an elimination reaction of 1,2-fluoroethene as precursor in an electrical discharge. The substance was identified and investigated by molecular beam Fourier transform microwave spectroscopy. Also fluorodiacetylene and with deuterium, D_2, as additional precursor fluoroacetylene-d1 and fluorodiacetylene-d1 were synthesized in the beam plasma. The hfs of the rotational transitions provided spin-rotation and deuterium nuclear quadrupole coupling constants. The experimental quadrupole coupling constants are compared to vibrationally corrected ab initio values.

Key words: Reactions and Syntheses in Electric Discharges; Nuclear Quadrupole and Spin-rotation Coupling; Molecular Beam Fourier Transform Microwave Spectroscopy; *ab initio* Calculations.

1. Introduction

In the following we report on the microwave rotational spectra of the fluoroacetylenes, FCCH, FCCD, and the fluorodiacetylenes, FCCCCH, FCCCCD. Molecular beam Fourier transform microwave spectroscopy (MBFTMW) was used to study their low-J spectra. To initiate their *in situ* synthesis from appropriate precursor molecules we have used a pulsed electric discharge within the nozzle of the spectrometer. The application of the discharge technique to MBFTMW spectroscopy has been introduced by Grabow, Heineking, and Stahl [1]. Subsequently it was used with great success by Gerry et al. [2, 3], Endo et al. [4], and Thaddeus et al. [5]. By this technique, new and possibly simpler syntheses can be carried out and the educt and product molecules can be studied also in excited vibrational states with high spectroscopic sensitivity [6] and resolution. The technique to trigger reactions by an electric discharge within the nozzle complements the techniques of pyrolysis [7] and laser photolysis [8, 9]. All three methods open new fields of research to microwave spectroscopy, since the spectra of even transient and thus otherwise elusive molecular species can be studied with kHz resolution.

The present study has been carried out in parallel to our corresponding investigation of carbonyl fluoride, F_2CO, ketene, H_2CCO, acetic acid, CH_3COOH, and the free radical difluorocarbene, CF_2, reported recently by us [10]. In the latter study we had proposed that F_2CO and H_2CCO are synthesized from F_2CCH_2 and CO_2 in a bimolecular reaction via an intermediate ring, and we expect that a similar but monomolecular and thus considerably more efficient reaction will take place if nitrosoalkenes are used as precursors. In such systems the inherent high sensitivity of the MBFTMW spectroscopy might even allow to intercept the four membered ring intermediates.

Our present study deals with the main reaction channel of F_2CCH_2, if subjected to an electrical discharge. It starts with the high yield monomolecular elimination of FH (see below).

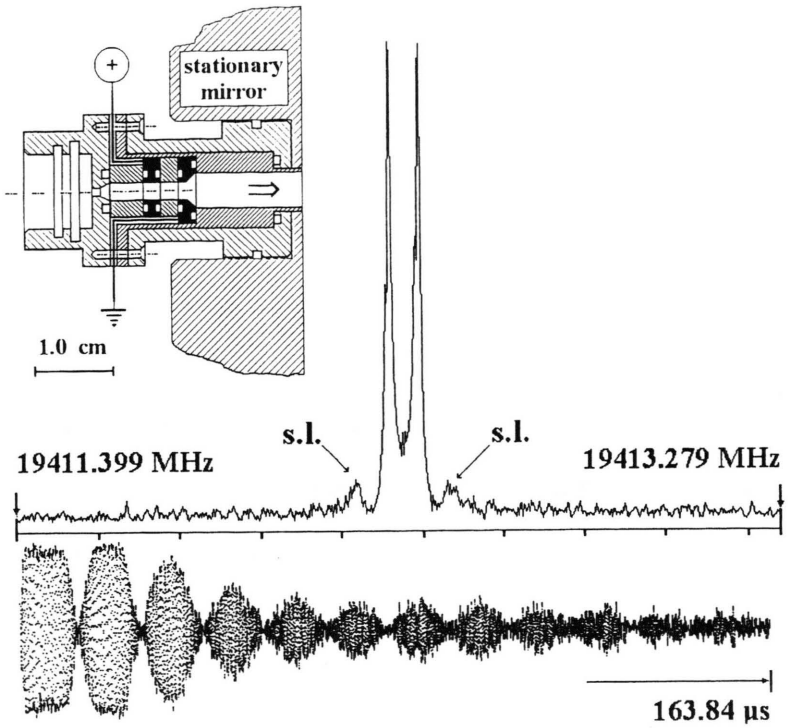

Fig. 1. A section of the amplitude spectrum of FCCH with the $J = 1 \rightarrow 0$ transition and the experimental time domain signal. 10 ns sampling interval, 4 averaging cycles, polarizing frequency 19412.34 MHz, 800 V discharge voltage. The saturation of the leading part of the free induction decay (lower trace) causes the side lobes (s.l.) in its Fourier transform spectrum. Insert: Cross section of the discharge nozzle designed by Grabow similar to [5].

2. Experimental

The measurements were performed with a MBFTMW spectrometer described in detail in [10].

We have used helium, neon, and predominantly argon as carrier gases with backing pressures between 1 and 1.5 bar.

The cooling effect and the tendency to form complexes are different for these rare gases. Thus a variation of the experimental conditions was possible. Mixtures of approximately 1 % of the precursors in the carrier gas have been used. Voltages of 700 to 1500 V were applied. The electrode near the nozzle mouth was kept on ground potential. This setting with the electrode upstream on positive potential proved slightly superior in the production of the investigated species. A cross-section of a preceeding design is shown in Fig. 2 of [5]. More experimental details will be given below, when different molecules are discussed.

3. Fluoroacetylene

With fluorobenzene, C_6H_5F, as precursor we got the first signal from the $J = 1 \rightarrow 0$ transition of fluoroacetylene, FCCH, at 19412.3 MHz, observed before by Laird and Tyler [11] . They had used absorption microwave spectroscopy with a discharge in the waveguide cell. Later experiments with 1,3,5-trifluorobenzene, $C_6H_3F_3$, trifluoromethylacetylene, CF_3CCH, and 1,1-difluoroethene, F_2CCH_2, improved the signal by magnitudes. The two last mentioned of these precursors have been used also in [11]. The best results were obtained with

Table 1. Hyperfine satellite frequencies (MHz) for the $J'' = 1 \rightarrow J' = 0$ rotational transition of FCCH. The hyperfine shifts, $\Delta\nu$, are defined as $\Delta\nu = \nu_{\text{satellite}} - \nu_{\text{center}}$, where ν_{center} designates the hypothetical transition frequency in the absence of the magnetic hyperfine interactions. To calculate the splittings we have used our program QSSR.FOR with $C_{\perp F} = 4.4$ kHz, $C_{\perp H} = -0.6$ kHz, and the direct spin-spin coupling constant $D_{F\cdots H} = -2.6$ kHz (see text). The limiting coupling scheme used to designate the states is $\hat{\boldsymbol{F}}_1 = \hat{\boldsymbol{J}} + \hat{\boldsymbol{I}}_F$; $\hat{\boldsymbol{F}} = \hat{\boldsymbol{F}}_1 + \hat{\boldsymbol{I}}_H$.

$J'' = 1 \rightarrow J' = 0$, $\nu_{\text{center}} = 19412.3539 \pm 0.0001$ MHz								
F''	(F_1'')	F'	(F_1')	ν_{obs}	$\Delta\nu_{\text{obs}}$	$\Delta\nu_{\text{calc}}$	$\nu_{\text{obs}} - \nu_{\text{calc}}$	int. [%]
2	3/2	1	1/2	19412.3563	.0024	.0025	–.0001	41.7
1	3/2	0	1/2	19412.3563	.0024	.0024	.0000	17.9
1	3/2	1	1/2	19412.3563	.0024	.0024	.0000	7.15
0	1/2	1	1/2	19412.3518	–.0021	–.0020	–.0001	8.33
1	1/2	0	1/2	19412.3480	–.0059	–.0059	.0000	7.15
1	1/2	1	1/2	19412.3480	–.0059	–.0059	.0000	17.9

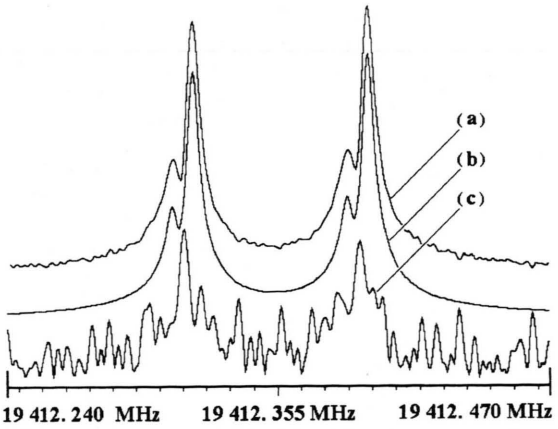

Fig. 2. A 250 kHz section of the amplitude spectrum of the $J = 1 \rightarrow 0$ transition of FCCH. Trace a: Experiment: 40 ns sampling interval, 16 k data points in the time domain, supplemented by 16 k zeros before Fourier transformation, 2048 averaging cycles, polarizing frequency 19412.35 MHz, 700 V discharge voltage. Trace b: Simulated spectrum fitting two components to the time domain signal. Trace c: Residuum revealing a third component with about 8 % of the intensity of the strongest component.

F_2CCH_2 as precursor, purchased from Fa. Aldrich, Steinheim.

We believe that FCCH is produced by the elimination reaction

$$F_2C{=}CH_2 \longrightarrow FC \equiv CH + HF. \qquad (1)$$

This reaction has been studied recently by Lin and Lee [12], who have used laser photolysis to energize the precursor. They detected hydrogen fluoride, HF, by step-scan time resolved Fourier transform infrared emission spectroscopy. Thereby the second elimination product of (1) was found. An efficient formation of HF from H and F radicals is unprobable, since three particle collisions would be required to shed off the excess energy, which are rare events in the beam.

By monitoring the signal intensity of the transition $J_{K-K+} = 1_{01} \rightarrow 0_{00}$ of the precursor, $F_2^{13}CCH_2$, at 15219.25 MHz with and without discharge, we estimated that roughly 50 % of the precursor molecule vanish under discharge. The isotopomer was used in natural abundance (1.1 %) to avoid saturation of the detection system.

We take this as a hint that a more effective discharge might improve the method. In Fig. 2 we give a reproduction of the $J = 1 \rightarrow 0$ transition of the most abundant species $F^{12}C^{12}CH$ with resolved spin-rotation splitting taken with 2048 measuring cycles, 16 k data points in the time domain, and 40 ns sampling interval. The polarizing conditions were chosen off-optimal, to avoid saturation of the detection system. Confining the measurement to the first part of the decay by 16 k data points and 10 ns sampling interval, the transition can be observed with reasonable signal to noise ratio already with one measuring cycle. Here the precursor F_2CCH_2 was exposed to a 1000 V discharge. This high intensity is demonstrated in Fig. 1, showing a measurement taken with four cycles. The side lobes in the FT spectrum result from the saturation of the detection system. The frequencies of the spin-rotation structure are given in Table 1 (compare too Figs. 2 - 4). They were obtained by a direct fit to the time domain signal [13 - 16], as the splittings are very narrow. Their analysis is given below. In Table 2 the frequencies of the $J = 1 \rightarrow 0$ transitions of $F^{13}CCH$ and $FC^{13}CH$ are included. They were measured with lower resolution in natural abundance. Here the spin-rotation hfs was not analyzed, since, with ^{13}C, these isotopomers contain an additional spin 1/2 nucleus.

To study the production process of FCCH in more detail we searched for the $J = 1 \rightarrow 0$ transitions of FCCH in excited vibrational states. With MBFTMW spectroscopy of stable species not produced by discharge it is usually difficult to observe rotational transitions in excited vibrational states, since the cooling process in the supersonic gas expansion tends to depopulate the higher vibrational states. By the investigation of the rotational spectra in vibrational excited states reported by Jones and Rudolph [17] and by Guarnieri [18] and by the IR-data of Holland et al. [19] we were able to detect and to measure the $J = 1 \rightarrow 0$ transitions of several excited vibrational states also given in Table 2. All existing transitions up to 1467 cm^{-1}, and in addition one in a state 2211 cm^{-1} above the ground state could be observed. For excited bending states with the quantum number $l \geq 1$ no rotational transition $J = 1 \rightarrow 0$ exists [20]. The search for the transitions $J = 1 \rightarrow 0$ in the states $v = 0011^11^1, \sum^-(2011.3\,cm^{-1})$ at 19413.8 MHz and $v = 0011^11^1, \sum^+(2015.0\,cm^{-1})$ at 19411.5 MHz near the ground state transition $v = 0000^00^0, \sum^+$ at 19412.3 MHz failed. The transitions $J = 1 \rightarrow 0$ in the states

$$v = 0003^11^1, \sum^+ \quad (2108.7\,cm^{-1}),$$

$$v = 0020^00^0, \sum^+ \quad (2108.1\,cm^{-1}),$$

$$v = 0011^11^1, \sum^- \quad (2011.3\,cm^{-1})$$

Table 2. Observed center frequencies ν_{obs} (MHz) for the $J'' = 1 \rightarrow J' = 0$ rotational transitions of $F^{13}CCH$, $FC^{13}CH$ in the vibrational ground state and of FCCH in excited vibrational states $v_1, v_2, v_3, v_4^{l_4}, v_5^{l_5}$. v_1: CH stretch, v_2: CC stretch, v_3: CF stretch, v_4: HCC bend, v_5: FCC bend, ν_{Lit} (MHz): previously reported values, G_v (cm^{-1}): vibrational excitation energies with respect to the vibrational ground state, $(S/N)_{norm}$: normalized signal to noise ratio (see text). In parentheses the mean error of several measurements is given.

$v_1\ v_2\ v_3\ v_4^{l_4}\ v_5^{l_5}$		ν_{obs}	ν_{Lit}	G_v	$(S/N)_{norm}$
$F^{13}CCH$:					
0 0 0 0 0	Σ^+	19401.2775	19401.12	0	0.66
$FC^{13}CH$:					
0 0 0 0 0	Σ^+	18747.8607	18747.94	0	0.62
FCCH:					
0 0 0 0 2^0	Σ^+	19521.1579(4)	19521.2	732.080	1.25
0 0 0 1^1 1^1	Σ^-	19485.5393(10)	19485.6	949.028	0.53
0 0 0 1^1 1^1	Σ^+	19483.9461(8)	19483.9	952.670	0.12
0 0 1 0 0	Σ^+	19338.0904(10)	19338.1	1061.445	0.81
0 0 0 2^0 0	Σ^+	19446.6525(15)	19446.6	1155.589	0.12
0 0 0 0 4^0	Σ^+	19624.7013(4)	–	1466.830	0.57
0 0 1 2^0 0	Σ^+	19378.9699(14)	19379.0	2211.614	< 0.1

could not be detected. All transitions in the excited states were measured with the same polarization and experimental conditions, but with different numbers n_c of averaging cycles. For comparison we give in Table 2 normalized signal to noise ratios $(S/N)_{norm} = (S/N)\, n_c^{-1/2}$ as a very rough measure of the number densities N_v of the species in the beam. Thus a comparison of the populations of the different vibrational states is approximately possible. $(S/N)_{norm}$ is also given for the ^{13}C-isotopomers. For the $J = 1 \rightarrow 0$ transition in the ground state of FCCH the $(S/N)_{norm}$ value could not be determined under these experimental conditions, because of the saturation of the detection system as shown in Figure 1. It can be assumed, that the reaction of (1) predominantly populates excited bending states of FCCH, since an elimination of HF starts with a bent FCCH structure. Unfortunately the $J = 1 \rightarrow 0$ transitions in the first bending states $v = 0000^01^1, \Sigma^-(366.6\ cm^{-1})$, FCC bend and $v = 0001^10^0, \Sigma^-(583.7\,cm^{-1})$, CCH bend do not exist [20]. One should look for the $J = 2 \rightarrow 1$ transitions near 39 GHz, which is beyond the range of our spectrometer. If one takes $(S/N)_{norm}$ as a measure of the number density in a state under consideration, Tab. 2 shows, that the second excited FCC bending state $v = 0000^02^0, \Sigma^+(732.1\,cm^{-1})$ is the most populated observable state within the supersonic beam.

Table 3. Rotational (B), centrifugal distortion (D_J), deuterium nuclear quadrupole coupling (χ_{aa}), spin-rotation coupling ($C_{\perp F}$, $C_{\perp H}$, and $C_{\perp D}$, resp.), and spin-spin ($D_{F\cdots H}$, $D_{F\cdots D}$, resp.) coupling constants for FCCH, FCCD, FCCCCH, and FCCCCD. Where applicable, the new values are compared to values reported in the literature. The spin-spin coupling constants are calculated from the experimental structures. They account only for the direct spin-spin coupling (see text).

FCCH	This work	[28]	[21]	[18]
B [MHz]	9706.1770(1)[a]	9706.19(2)	–	9706.18459(4)[a]
$C_{\perp F}$ [kHz]	4.4(6)	–	< 8	–
$C_{\perp H}$ [kHz]	–0.6(2)	–	< 8	–
$D_{F\cdots H}$ [kHz]	–2.6	–	–	–

FCCD	This work	[32]	[29]	[32]	[30]
B [MHz]	8736.0225(6)	8736.04(2)	–	8736.06(-)	–
χ_{aa} [kHz]	210.9(14)	–	212(10)	–	205.4(12)
$C_{\perp F}$ [kHz]	3.6(9)	–	–	–	
$C_{\perp D}$ [kHz]	–0.6(4)	–	–	–	
$D_{F\cdots D}$ [kHz]	–0.39	–	–	–	

FCCCCH[d]	This work	[36]	[35]
B [MHz]	2038.09840(14)[b]	2038.09791(10)	2038.098(24)
D_J [kHz]	0.08459(18)	0.084194(36)	0.0846(34)

FCCCCD[d]	This work	[36]	[35]
B [MHz]	1927.49234(16)[c]	1927.49128(112)	
D_J [kHz]	0.07383(10)	0.0790390(303)	0.0846(34)
χ_{aa} [kHz]	206.2(10)	–	

[a] The difference results from the neglect of centrifugal distortion included in [18]; [b] measurements of [35, 36] included; [c] measurements of [36] included; [d] magnetic interactions, i.e. $C_{\perp F}$, $C_{\perp D}$, $D_{F\cdots H}$, $D_{F\cdots D}$ neglected.

4. Analysis of the Spin-rotation Splitting

By using MW Stark spectroscopy with an oversized L-band Stark cell, Weiss et al. [21] obtained a half width at half height of 8 kHz for the $J = 1 \rightarrow 0$ transition of FCCH and estimated an upper limit for the spin-rotation constants of 8 kHz for $|M_{bb}^F|$ and $|M_{bb}^H|$. Only a line broadening, no splitting could be observed in their experiments. It should be noticed, that the definition of the spin-rotation constants M and C differs in sign [22, 23]. As shown in Fig. 2 MBFTMW spectroscopy clearly reveals a doublet structure with a half width at half height of 4.5 kHz for the larger component, taken from the FT amplitude spectrum. With two spin 1/2 nuclei a quartet structure is expected.

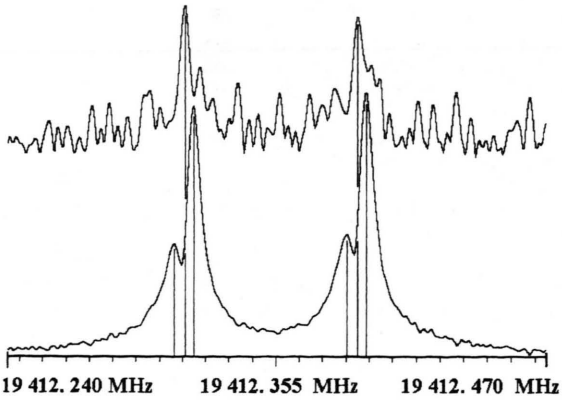

Fig. 3. Visualization of the position of the residuum signal between the two stronger components.

First a doublet structure was fitted to the time domain signal. The residuum of this fit revealed an additional component of roughly 8 % of the strongest component. This is illustrated in Fig. 2 by the lower trace c. Figure. 3 shows, that this component is positioned between the two visible components.

The frequencies of the three components are

$$\nu_1 = 19412.3479\,\text{MHz},$$

$$\nu_2 = 19412.3519\,\text{MHz},$$

$$\nu_3 = 19412.3562\,\text{MHz}.$$

They are taken as experimental basis for the determination of the spin-rotation interaction. For the analysis the effective Hamiltonian, $\hat{H}$ in frequency units was chosen as

$$\hat{H} = \hat{H}_\text{R} + \hat{H}_\text{CENT} + \hat{H}_\text{SR} + \hat{H}_\text{SS} \tag{2}$$

with

$$\hat{H}_\text{R} = B\hat{\boldsymbol{J}}^2 \tag{3}$$

as rigid rotor part, B the rotational constant, and $\hat{\boldsymbol{J}}$ the angular momentum operator in units of $\hbar$. The centrifugal distortion

$$\hat{H}_\text{CENT} = D_J\hat{\boldsymbol{J}}^4 \tag{4}$$

was neglected for FCCH and FCCD. For the latter the operator $\hat{H}_Q$ for the electric nuclear quadrupole coupling for the deuterium hfs will be added later.

In the following we use a notation for an asymmetric top. Later it will be reduced to a linear molecule.

The spin-rotation coupling, which is caused by the interaction of the magnetic field produced by the rotating charges of the molecule and the nuclear magnetic moment is described in matrix notation by

$$\hat{H}_\text{SR} = \sum_{i=F,H} \hat{\boldsymbol{I}}_i \cdot C_i \cdot \hat{\boldsymbol{J}}^\dagger, \tag{5}$$

where $\hat{\boldsymbol{I}}_i$ are the nuclear spin operators in units of $\hbar$, here for the nuclei F and H, and C_i is a cartesian spin-rotation coupling tensor. † denotes the transposed matrix.

$$C_i = \begin{pmatrix} C_{aa,i} & C_{ab,i} & C_{ac,i} \\ C_{ba,i} & C_{bb,i} & C_{bc,i} \\ C_{ca,i} & C_{cb,i} & C_{cc,i} \end{pmatrix}. \tag{6}$$

When for $\hat{\boldsymbol{I}}_i = \left(\hat{I}_{Xi}, \hat{I}_{Yi}, \hat{I}_{Zi}\right)$ space fixed components, for $\hat{\boldsymbol{J}} = \left(\hat{J}_{ai}, \hat{J}_{bi}, \hat{J}_{ci}\right)$ molecule fixed coordinates are used and the cartesian tensor components are referred to the molecule fixed axes a, b, c, (5) should be rewritten in the symmetrized form

$$\hat{H}_\text{SR} = \frac{1}{2}\left(\sum_{i=F,H}\left(\hat{\boldsymbol{I}}_i \cdot \hat{\Phi} \cdot C_i \cdot \hat{\boldsymbol{J}}^\dagger\right) + \left(\hat{\boldsymbol{I}}_i \cdot \hat{\Phi} \cdot C_i \cdot \hat{\boldsymbol{J}}^\dagger\right)^\dagger\right). \tag{7}$$

The first two factors represent the components of the spin $\hat{\boldsymbol{I}}_i$ in the molecule fixed axes.

$$\hat{\Phi} = \begin{pmatrix} \hat{\Phi}_{Xa} & \hat{\Phi}_{Xb} & \hat{\Phi}_{Xc} \\ \hat{\Phi}_{Ya} & \hat{\Phi}_{Yb} & \hat{\Phi}_{Yc} \\ \hat{\Phi}_{Za} & \hat{\Phi}_{Zb} & \hat{\Phi}_{Zc} \end{pmatrix}. \tag{8}$$

The $\hat{\Phi}_{Fg}$ are the direction cosines between the space fixed axes $F = X, Y, Z$ and the molecule fixed system $g = a, b, c$.

For a truly symmetric top molecule the off diagonal elements of C_i vanish by symmetry and $C_{bb,i} = C_{cc,i} = C_{\perp,i}$. For a linear molecule, $\hat{H}_\text{SR}$ further reduces to

$$\hat{H}_\text{SR} = \sum_{i=F,H} C_{\perp i} \cdot \hat{\boldsymbol{I}}_i \cdot \hat{\boldsymbol{J}}. \tag{9}$$

For the direct spin-spin interaction, $\hat{H}_\text{SS}$, caused by the magnetic moments of the nuclei j and k (j, k = F, H, D, respectively) we use [24]

$$\hat{H}_{SS} = \hat{\boldsymbol{I}}_j \cdot \hat{D}_{(j\cdots k)} \cdot \hat{\boldsymbol{I}}_k. \tag{10}$$

Referred to the space fixed cartesian axes system, the traceless spin-spin coupling tensor, $\hat{D}_{(j\cdots k)\,FF'}$ has the elements

$$\hat{D}_{(j\cdots k)\,FF'} = -\left(\frac{\beta^2}{h}\right) \cdot \left(\frac{\mu_j \mu_k}{I_j I_k}\right) \cdot \frac{1}{r_{j,k}^3} \left(\frac{3}{2}\left(\hat{\Phi}_{aF}\hat{\Phi}_{aF'} + \hat{\Phi}_{aF'}\hat{\Phi}_{aF}\right) - \delta_{FF'}\right). \tag{11}$$

In (11) $\hat{\Phi}_{aF}$, $\hat{\Phi}_{aF'}$ are the direction cosines between the molecular axis and the space fixed F-axis and F'-axis, respectively (F or $F' = X, Y, Z$). I_j and I_k are the nuclear spins. μ_j and μ_k are the nuclear magnetic moments in units of the nuclear magneton β ($\mu_F = 2.6287$, $\mu_H = 2.79278$, $\mu_D = 0.85742$ [25]). r_{jk} is the distance between the two interacting nuclei.

We used the programs QSSR.FOR and QSSRFIT.FOR [26], in which the hamiltonian is set up in spherical tensor notation [27]. The hamiltonian matrices are treated in the coupling scheme:

$$\hat{\boldsymbol{I}}_F + \hat{\boldsymbol{I}}_H = \hat{\boldsymbol{I}}, \quad \hat{\boldsymbol{I}} + \hat{\boldsymbol{J}} = \hat{\boldsymbol{F}} \tag{12}$$

and numerically diagonalized. In the tables however, we use the coupling scheme

$$\hat{\boldsymbol{J}} + \hat{\boldsymbol{I}}_1 = \hat{\boldsymbol{F}}_1, \quad \hat{\boldsymbol{F}}_1 + \hat{\boldsymbol{I}}_2 = \hat{\boldsymbol{F}} \tag{13}$$

to label the satellites, where the index 1 refers to the nucleus which is coupled more strongly to the overall rotation. The rotational constant B and the spin-rotation constants $C_{\perp F}$ and $C_{\perp H}$ could be determined.

The direct spin-spin coupling constants

$$Dj\cdots k = -\left(\frac{\beta^2}{h}\right) \cdot \left(\frac{\mu_j \mu_k}{I_j I_k}\right) \frac{1}{r_{j,k}^3}$$

for the monoacetylenes were calculated from the distance $r_{FH} = 3.53$ Å [28] between the F and H atoms, the nuclear magnetic moments, and the nuclear spins as

$$D_{F\cdots H} = -2.6\ \text{kHz} \quad \text{for} \quad FCCH,$$

$$D_{F\cdots D} = -0.39\ \text{kHz} \quad \text{for} \quad FCCD.$$

They were kept constant in the fitting calculations.

At first glance, only a doublet can be seen in Figure 2. With the procedure described above, a third weak component was detected. The question arose, how to distribute the four components with the relative intensities 41.667 %, 25 %, 25 %, and 8,333 % suggested by theory with the selection rules $\Delta J = 1$, $\Delta I = 0$, $\Delta F = \pm 1, 0$. By plausibility we assigned the strongest component $J,\ F,\ F_1 = 1,\ 2,\ 3/2 \rightarrow 0,\ 1,\ 1/2$ with the relative intensity 41.7 % to the strong component at the higher frequency and assigned the component $1,\ 1,\ 3/2 \rightarrow 0,\ 0,\ 1/2$ with 25 % relative intensity in addition to it. The component $1,\ 1,\ 1/2 \rightarrow 0,\ 1,\ 1/2$ (25 % rel. intens.) was assigned to the weaker low frequency component of Figure 2. Finally, the $1,\ 0,\ 1/2 \rightarrow 0,\ 1,\ 1/2$ component with the theoretical relative intensity of 8.3 % was assigned to the hidden, central component. A fit resulted in a mean squares deviation in the order of 0.1 kHz. Moving the $1,\ 0,\ 1/2 \rightarrow 0,\ 1,\ 1/2$ component to the higher or lower visible component of Fig. 2 increased the mean square deviation to about 1 kHz. This convinced us that the assignment given in Table 1 is reasonable. The resulting molecular constants are given in Table 3. In Fig. 4 a synthesized line shape, calculated within the short pulse approximation [14] from the fitted molecular constants, theoretical intensities, and the molecular velocity in the supersonic beam, is given together with the corresponding bar spectrum and is compared to the measured line profile.

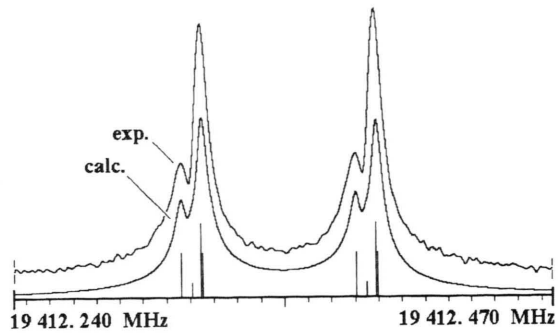

Fig. 4. Comparison of the experimental spectrum trace a in Fig. 2 and a simulated spectrum calculated with the four components indicated by bars.

5. Fluoroacetylene-d1

Fluoracetylene-d1, FCCD, was first investigated by Tyler and Sheridan [28]. The D-hfs was reported in [29] and in [30]. In [30] waveguide FTMW spectroscopy was applied, but the hfs-analysis did not include spin- rotation and spin-spin interaction. Further contributions are found in [17, 31, 32]. Thus the

Table 4. Hyperfine satellite frequencies (MHz) for the $J'' = 1 \rightarrow J' = 0$ rotational transition of FCCD. The hyperfine shifts are defined as $\Delta\nu = \nu_{\text{satellite}} - \nu_{\text{center}}$, where ν_{center} designates the hypothetical transition frequency in the absence of all magnetic hyperfine interactions. The limiting coupling scheme used to designate the states is $\hat{\boldsymbol{F}}_1 = \hat{\boldsymbol{J}} + \hat{\boldsymbol{I}}_D$; $\hat{\boldsymbol{F}} = \hat{\boldsymbol{F}}_1 + \hat{\boldsymbol{I}}_F$. In brackets the mean error of eight measurements is given.

$J'' = 1 \rightarrow J' = 0$, $\nu_{\text{center}} = 17472.0447$ MHz								
F''	(F_1'')	F'	(F_1')	ν_{obs}	$\Delta\nu_{\text{obs}}$	$\Delta\nu_{\text{calc}}$	$\nu_{\text{obs}} - \nu_{\text{calc}}$	int. [%]
3/2	1	3/2	1	17472.0977(1)	.0530	.0541	−.0011	17.8
3/2	1	1/2	1	17472.0977(1)	.0530	.0541	−.0011	4.38
1/2	1	1/2	1	17472.0977(1)	.0530	.0519	.0011	7.61
1/2	1	3/2	1	17472.0977(1)	.0530	.0519	.0011	3.51
5/2	2	3/2	1	17472.0367(2)	−.0080	−.0093	.0013	33.3
3/2	2	1/2	1	17472.0300(5)	−.0147	−.0140	−.0006	17.8
3/2	2	3/2	1	17472.0300(5)	−.0147	−.0140	−.0006	4.38
1/2	0	3/2	1	17471.9404(1)	−.1043	−.1043	.0000	7.61
1/2	0	1/2	1	17471.9404(1)	−.1043	−.1043	.0000	3.51

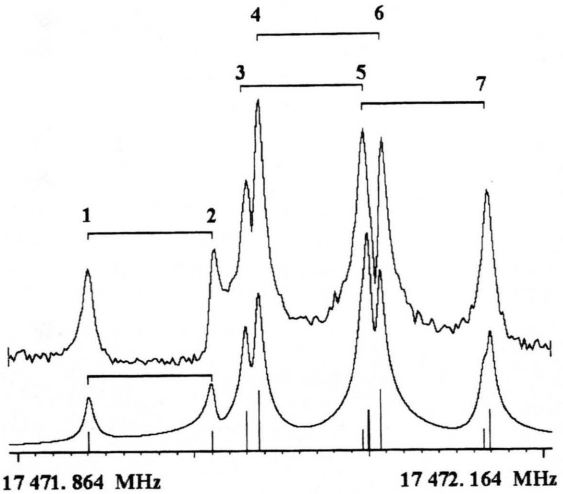

Fig. 5. A section of the amplitude spectrum of the $J = 1 \rightarrow 0$ transition of FCCD produced by discharge from $CF_2CH_2 + D_2$ (upper trace)and a simulated spectrum with bars indicating the hfs components (lower trace). The square brackets indicate the Doppler doublets. 10 ns sampling interval, 16 k data points in the time domain, supplemented by 16 k zeros prior to Fourier transformation, 8192 averaging cycles, polarizing frequency 17471.98 MHz, 1500 V discharge voltage.

$J = 1 \rightarrow 0$ transition of FCCD could be detected easily. For the production of the deuterated species we used F_2CCH_2 and D_2 with 0.8 % and 1.6 %, respectively, in argon. The backing pressure was 1.1 bar, the discharge voltage 1500 V. The other experimental data are included in the caption of Figure 5. Here the deuterium nuclear quadrupole coupling is the main source for the hyperfine structure. The spin-rotation interaction is most clearly seen by the splitting of the Doppler components 3 and 4 of Figure 5. In the Doppler components 5 and 7 several hfs-components overlap. The frequencies used for the analysis were again obtained by a direct fit to the time domain signal and are given in Table 4.

For the analysis of the D-hfs the hamiltonian in frequency units (2) has to be supplemented by

$$H_Q = -(1/6h)\ \mathbf{Q} : \boldsymbol{\nabla}\mathbf{E} \tag{14}$$

expressed in dyadic form [33, 34] in a space fixed reference system. $\mathbf{Q}$ is the nuclear quadrupole dyad and $\boldsymbol{\nabla}\mathbf{E}$ the dyad for the electric field gradient. For a linear molecule $\chi_{aa} = |e|Qq_{aa}/h$ remains as adjustable parameter, with $|e|Q$ the nuclear quadrupole moment, e the electronic charge, and q_{aa} the second derivative of the Coulomb potential V, caused by the extranuclear charge distribution. Again the programs QSSR.FOR and QSSRFIT.FOR were used for the analysis. The molecular constants are given in Table 3.

6. Fluorodiacetylene

In the course of our measurements of FCCH, under conditions mentioned before, we noticed, that also fluorodiacetylene, FCCCCH, is produced. The investigations, published by Okabayashi et al. [35] and Dore et al. [36], helped us to assign the measured lines. With the exception of one line these authors report only high J transitions with $J \geq 12$. Our results are given in Table 4. They include one transition of a ^{13}C-isotopomer. Within the resolution of our spectrometer the lines did not show any indication of

Table 5. Frequencies ν_{obs} of low J transitions of FCCCCH and FCC^{13}CCH and comparison with earlier results, $\nu_{\text{obs}}^{\text{Lit}}$, reported in [36]. $\Delta\nu = \nu_{\text{obs}} - \nu_{\text{calc}}$. The narrowly spaced hyperfine multiplets caused by the magnetic spin-rotation and spin-spin interactions of the spin-(1/2) nuclei could not be resolved.

Molecule	$J'' \rightarrow J'$	ν_{obs} / MHz	$\Delta\nu$ / kHz	$\nu_{\text{obs}}^{\text{Lit}}$
FCCCCH	$1 \rightarrow 0$	4076.1966	< 1	–
	$2 \rightarrow 1$	8152.3905	< 1	–
	$3 \rightarrow 2$	12228.5810	< 1	12228.587
	$4 \rightarrow 3$	16304.7646	< 1	–
FCC^{13}CCH	$3 \rightarrow 2$	12116.2995	–	–

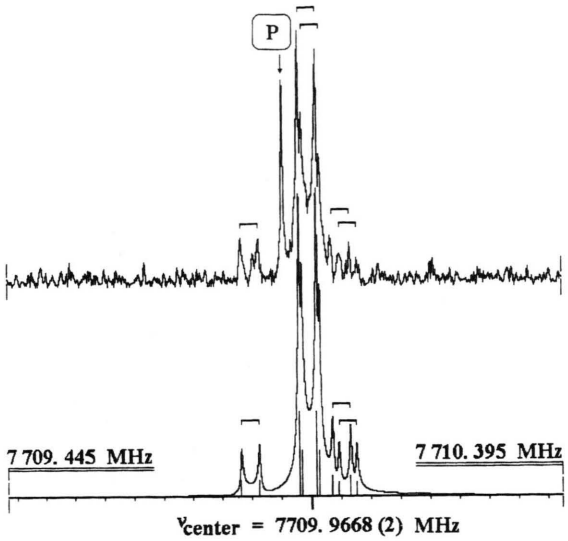

Fig. 6. A section of the amplitude spectrum of the $J = 2 \rightarrow 1$ transition of FCCCCD produced by discharge from $CF_2CH_2 + D_2$ (upper trace). Simulated spectrum with bars indicating the hfs components (lower trace). The square brackets indicate the Doppler doublets. 20 ns sampling interval, 16 k data points in the time domain, supplemented by 16 k zeros prior to Fourier transformation, 24234 averaging cycles, polarizing frequency 7709.92 MHz, 1100 V discharge voltage.

a hyperfine structure. This is in agreement with an estimate of the spin-rotation and spin-spin coupling constants, which must have values below 1 kHz, as will be discussed later. The results of a centrifugal distortion analysis, which also includes the lines of [35] and [36], are given in Table 3. The detection of FCCCCH clearly demonstrates that molecules are not only cracked into smaller fragments within the discharge, but that such fragments are also quite effectively assembled to longer chain molecules.

7. Fluorodiacetylene-d1

Fluorodiacetylene-d1, FCCCCD, was produced in a discharge similar to the production of FCCD. 1 % F_2CCH_2 and 2 % D_2 in argon were exposed to a discharge with 1100 V at backing pressures between 1.1 to 1.5 bar. In [36] a production of FCCCCD is described by using pentafluorostyrene, $C_6F_5CHCH_2$, and D_2 as precursors in a dc glow discharge. Rotational transitions with $J = 25$ to $J = 52$, and the rotational constant B and the centrifugal distortion constant D_J were reported. We measured the rotational transitions $J = 1 \rightarrow 0$ to $J = 4 \rightarrow 3$. The D-hfs was observed and analyzed for the two lowest transitions. They are given in Table 6. Unfortunately we could not clearly measure the weakest component of the $J = 1 \rightarrow 0$ transition, although we averaged the time domain signal by 24000 experiment cycles, which is near the limit (32 k) of our instrument.

As in the case of FCCCCH a down scaling of the spin-rotation and spin-spin coupling constants of FCCH and FCCD showed us that in FCCCCD these constants must be less than 1 kHz. So the hfs-structure given in Table 6 was analyzed as produced by electric nuclear quadrupole coupling. The hamiltonians (2) and (14) provided the basis. Again the programs QSSR.FOR and QSSRFIT.FOR were used. The rotational constant B and the coupling parameter $\chi_{aa} = |e|Qq_{aa}/h$ were fitted and are given in Table 3.

Table 6. Observed hyperfine satellite transition frequencies (in MHz) for FCCCCD . The hyperfine shifts are defined as $\Delta\nu = \nu_{\text{satellite}} - \nu_{\text{center}}$. The limiting coupling scheme used to designate the states is: $\hat{\boldsymbol{F}}_1 = \hat{\boldsymbol{J}} + \hat{\boldsymbol{I}}_D$; $\hat{\boldsymbol{F}} = \hat{\boldsymbol{F}}_1 + \hat{\boldsymbol{I}}_F$. All magnetic hyperfine interaction were neglected in the calculations.

$J'' = 1 \rightarrow J' = 0$, $\nu_{\text{center}} = 3854.9832$ MHz								
F''	(F_1'')	F'	(F_1')	ν_{obs}	$\Delta\nu_{\text{obs}}$	$\Delta\nu_{\text{calc}}$	$\nu_{\text{obs}} - \nu_{\text{calc}}$	int. [%]
3/2	1	1/2	1	3855.0336	.0504	.0514	−.0015	3.70
3/2	1	3/2	1	3855.0336	.0504	.0514	−.0010	18.5
1/2	1	1/2	1	3855.0336	.0504	.0514	−.0010	7.41
1/2	1	3/2	1	3855.0336	.0504	.0514	−.0010	3.70
5/2	2	3/2	1	3854.9739	−.0093	−.0103	.0010	33.3
3/2	2	1/2	1	3854.9739	−.0093	−.0103	.0010	18.5
3/2	2	3/2	1	3854.9739	−.0093	−.0103	.0010	3.70
$J'' = 1 \rightarrow J' = 0$, $\nu_{\text{center}} = 7709.9671$ MHz								
F''	(F_1'')	F'	(F_1')	ν_{obs}	$\Delta\nu_{\text{obs}}$	$\Delta\nu_{\text{calc}}$	$\nu_{\text{obs}} - \nu_{\text{calc}}$	int. [%]
5/2	2	5/2	2	7710.0301	.0630	.0624	.0007	4.67
3/2	2	3/2	2	7710.0301	.0630	.0615	.0015	3.00
3/2	1	1/2	0	7710.0170	.0499	.0523	−.0024	3.70
1/2	1	1/2	0	7710.0170	.0499	.0501	−.0001	7.41
5/2	2	3/2	1	7709.9671	.0000	.0006	−.0005	15.0
3/2	2	1/2	1	7709.9671	.0000	−.0008	.0008	8.34
3/2	2	3/2	1	7709.9671	.0000	−.0015	.0016	1.67
7/2	3	5/2	2	7709.9622	−.0049	−.0041	−.0008	26.7
5/2	3	3/2	2	7709.9622	−.0049	−.0052	.0003	18.7
5/2	3	5/2	2	7709.9622	−.0049	−.0065	.0016	1.33
3/2	1	1/2	1	7709.8638	−.1033	−.1011	−.0022	0.93
3/2	1	3/2	1	7709.8638	−.1033	−.1018	−.0014	4.63
1/2	1	1/2	1	7709.8638	−.1033	−.1034	.0001	1.85
1/2	1	3/2	1	7709.8638	−.1033	−.1041	.0009	0.93

8. Discussion

8.1. Spin-rotation Coupling

Since we were able to determine the spin-rotation constants given in Table 3, and since the high resolution of MBFTMW spectroscopy promises more results in near future, we want to discuss a method to estimate their values on the basis of known constants.

According to [37, 22] the spin-rotation constants of linear molecules are proportional to the rotational constant B and the dimensionless gyromagnetic ratio or g factor [38] of the nucleus under consideration.

$$g_I = \frac{\mu_I}{\beta \cdot I} \tag{15}$$

with μ_I the nuclear magnetic moment, β the nuclear magneton and I the nuclear spin.

Explicitly DeLucia and Gordy [39] used the relation

$$C_{\perp \mathrm{H}} = \frac{B_{\mathrm{HCN}}}{B_{\mathrm{DCN}}} \frac{g_{\mathrm{H}}}{g_{\mathrm{D}}} C_{\perp \mathrm{D}} \tag{16}$$

to estimate the unknown constant $C_{\perp \mathrm{H}}$ for HCN with the help of the known values for DCN of the right hand side of (16). With the help of detailed considerations given by Flygare [22], (16) may be verified. The essential statement written in our nomenclature is

$$C_{gg,i} = \frac{\mu_i}{I_i I_{gg}} (\Sigma_1 + \Sigma_2) \tag{17}$$

with $C_{gg,i}$ the gg component of the spin-rotation coupling tensor (6) of the nucleus i, μ_i its nuclear magnetic moment and I_i its nuclear spin. For I_{gg} we take the principal moments of inertia of the molecule as an approximation. Σ_1 depends on the nuclear charges and the geometry of the molecule, Σ_2 on the electronic charge distribution, mainly near the nucleus under consideration, i.e. on the position of the electrons in the molecule, and on electronic angular momenta and energies. Σ_1 and Σ_2 compensate each other to a great extend. Provided that $(\Sigma_1 + \Sigma_2)$ are equal for two molecules to be compared, (16) is strictly valid. Otherwise (16) is an approximation.

We tested the approximation for the prediction of $C_{gg,i}$ of the following pairs of molecules:

Table 7. Estimates of spin-rotation coupling constants in analogy to (16). The experimental values of HF, DF, and HC_2F are the basis for these calculations. The errors of the estimated values were calculated by error propagation and do not include errors of the approximation. B rotational constant. $C_{\perp i} = C_i$, i = H, D, F spin-rotation coupling constant. X = H or D as applicable. n. o. means no splitting observed.

Molecule	B [MHz]	$C_{\mathrm{F,exp}}$ [kHz]	$C_{\mathrm{F,pred}}$ [kHz]	$C_{\mathrm{H,exp}}$ [kHz]	$C_{\mathrm{H,pred}}$ [kHz]
HF	616365.200(10)[a]	307.637(20)[c]	—	−71.128(24)[c]	—
HC_2F	9706.1770(1)	4.4(6)	4.844(3)	−0.6(2)	−1.120(4)
HC_4F	2038.09840(14)	n.o.	1.0172(1)	n.o.	−0.2352(6)
Molecule	**B [MHz]**	**$C_{\mathrm{F,exp}}$ [kHz]**	**$C_{\mathrm{F,pred}}$ [kHz]**	**$C_{\mathrm{D,exp}}$ [kHz]**	**$C_{\mathrm{D,pred}}$ [kHz]**
DF	325584.980(300)[b]	158.356(45)[c]	—	−5.755(19)[c]	—
DC_2F	8736.0225(6)	3.6(9)	4.249(1)	−0.6(4)	−0.1544(5)
DC_4F	1927.49234(16)	n.o.	0.9375(3)	n.o.	−0.0341(1)
Molecule	**B [MHz]**	**$C_{\mathrm{F,exp}}$ [kHz]**	**$C_{\mathrm{F,pred}}$ [kHz]**	**$C_{\mathrm{X,exp}}$ [kHz]**	**$C_{\mathrm{D,pred}}$ [kHz]**
HC_2F	9706.1770(1)	4.4(6)	—	−0.6(2)	—
DC_2F	8736.0225(6)	3.6(9)	4.0(5)	−0.6(4)	-0.08(3)
Molecule	**B [MHz]**	**$C_{\mathrm{F,exp}}$ [kHz]**	**$C_{\mathrm{F,pred}}$ [kHz]**	**$C_{\mathrm{D,exp}}$ [kHz]**	**$C_{\mathrm{D,pred}}$ [kHz]**
DC_2F	8736.0225(6)	3.6(9)	—	−0.6(4)	—
DC_4F	1927.49234(16)	n.o.	0.8(2)	n.o.	−0.1(1)
Molecule	**B [MHz]**	**$C_{\mathrm{F,exp}}$ [kHz]**	**$C_{\mathrm{F,pred}}$ [kHz]**	**$C_{\mathrm{H,exp}}$ [kHz]**	**$C_{\mathrm{H,pred}}$ [kHz]**
HC_2F	9706.1770(1)	4.4(6)	—	−0.6(2)	—
HC_4F	2038.09840(14)	n.o.	0.9(1)	n.o.	-0.13(4)

[a] [40]; [b] [41]; [c] [42].

$$\mathrm{HF} \mapsto \mathrm{HCCF},$$

$$\mathrm{HF} \mapsto \mathrm{HCCCCF},$$

$$\mathrm{DF} \mapsto \mathrm{DCCF},$$

$$\mathrm{DF} \mapsto \mathrm{DCCCCF},$$

$$\mathrm{HCCF} \mapsto \mathrm{DCCF},$$

$$\mathrm{DCCF} \mapsto \mathrm{DCCCCF},$$

$$\mathrm{HCCF} \mapsto \mathrm{HCCCCF}.$$

The results are given in Table 7.

It can be seen, that the predicted values $C_{i,\mathrm{pred}}$, i = H, D, F agree surprisingly well with with the experimental values C_{exp}. That means that (16) may be used as a guide in further investigations, provided that the close vicinity of the nucleus under consideration is sufficiently similar in both molecules. But the prediction cannot replace the experimental evaluation.

8.2. D-hfs

8.2.1. General Remarks

The spectroscopic coupling constant, χ_{aa}, relates to the anisotropy in the intramolecular electric field gradient tensor at the position of the deuterium nucleus as

$$\chi_{aa} = \frac{e^2 Q_D}{a_o^3 h} \cdot \left(V_{aa} - \frac{V_{aa} + V_{bb} + V_{cc}}{3} \right). \quad (18)$$

Here V_{aa}, V_{bb}, V_{cc} designate the second derivatives of the intramolecular Coulomb potential (in atomic units) as caused by the charge distribution of the other nuclei and the electrons.

The potential terms in the parentheses of (18) represent $\partial^2 V/\partial g^2$ with $g = a, b, c$ at the nucleus as caused by the *extranuclear* molecular charge distribution. At least in principle, the values V_{aa}, V_{bb}, V_{cc} can be calculated by ab initio methods. Q_D, e, a_o, h are the quadrupole moment of the deuterium nucleus, the electronic charge, Bohr's radius, and Planck's constant, respectively. The slight difference in the experimental values for the deuterium nuclear quadrupole coupling constant in FCCD and FCCCCD correlates to the slightly shorter r_{CD} bond distance in FCCD. The shorter the bond distance, the higher the value of the quadrupole coupling constant. (Compare too the extensive ab initio studies of deuterium quadrupole coupling constants carried out by Huber and coworkers [43 - 45]).

Already a standard ab initio calculation of the second derivatives V_{aa} etc., in our case a MP2/6-31G(d,p) calculation carried out with the GAUSSIAN 94 suite of programs [46], reproduces the *difference* between the deuterium coupling constants of FCCD and FCCCCD almost quantitatively. However these ab initio values are systematically too high by about thirteen percent. The reason for this is twofold. First, the experimental values should be compared to vibronic expectation values for the ab initio quadrupole coupling constants rather than to values calculated at the energy relaxed equilibrium configurations. Second, the quality of the ab initio calculation might need refinement, i.e one might need to account better for electron correlation (to go beyond second order Møller-Plesset perturbation theory, MP2 [47]) and, probably more important, especially in the case of the atom containing the quadrupole nucleus, here the deuterium, one should use a more flexible set of atomic basis functions. In the following we will look into both aspects in more detail.

8.2.2. Vibrational Corrections

In order to get at least an estimate for the vibrational corrections, we have used the local mode model pushed to its extreme. For both molecules we have treated the heavy atoms (F and C) as frozen to their positions in the linear, energy relaxed, equilibrium configuration of the ab initio calculation. In other words, only the deuterium atom was allowed to vibrate. Furthermore we have approximated the vibrational modes of the deuterium atom as a CD stretching mode and a pure (degenerate) bending mode with the CD bond distance fixed to its value in the linear equilibrium configuration. We will treat the stretching mode first.

8.2.3. CD-stretching Correction

Within the frame of our frozen heavy atom chain model the Schrödinger equation for the deuterium stretching vibration takes the form

$$-\frac{\hbar^2}{2m_D} \frac{d^2\Psi(x)}{dx^2} + V(x)\Psi(x) = E\Psi(x). \quad (19)$$

Here x denotes the deviation of the instantaneous CD-bond distance from its equilibrium value and m_D denotes the mass of the deuterium atom. As vibrational potential, $V(x)$, we have chosen a Morse-potential. With only two adjustable parameters it leads to a quite accurate approximation of the ab initio potential curve for a comparatively large range of x-values:

$$V(x) = D\left(e^{-a\,x} - 1\right)^2. \quad (20)$$

In the present application we have adjusted the parameters a and D to the single point ab initio ground state energies, E^{MP2}, calculated at $r_{CD}^{(eq)}$ and at $r_{CD}^{(eq)} \pm \Delta x$ with $\Delta x = 0.12$ Å as

$$a = \frac{1}{\Delta x} \ln\left(\left(\frac{E^{MP2}(-\Delta x) - E^{MP2}(0)}{E^{MP2}(+\Delta x) - E^{MP2}(0)} \right)^{1/2} \right) \quad (21)$$

and

$$D = \left(E^{MP2}(-\Delta x) - E^{MP2}(0)\right) / \left(e^{a\cdot\Delta x} - 1\right)^2. \quad (22)$$

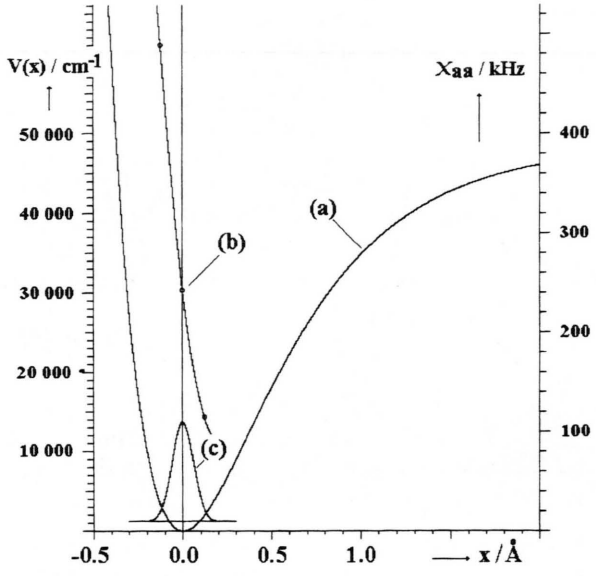

Fig. 7. MP2/6-31G(d,p) results for the pure CD-stretching vibration (see text). Trace a: Morse potential V, adapted to the ab initio energies at $x = 0$ Å and $x = \pm 0.12$ Å. Trace b: x-dependance of the deuterium coupling constant χ_{aa}. Trace c: Probability density for the deuterium nucleus $|\Psi(x)|^2$. Within the resolution of the figure it is hardly possible to discriminate between these results and those obtained with the enlarged basis sets.

For the approximation of the x-dependence of the quadrupole coupling constant, $\chi_{aa} = \chi(x)$, we have used a Taylor polynomial of second order in x:

$$\chi(x) = \chi(0) + \chi_x \cdot x + \frac{\chi_{xx}}{2} x^2. \tag{23}$$

Here, in principle, χ_x and χ_{xx} denote the first and second derivative of $\chi(x)$ at the equilibrium position $x = 0$. In practice, however, we have adjusted the values of $\chi(0)$, χ_x, χ_{xx} to the MP2/6-31G(d,p) values calculated at $x = -0.12$ Å, $x = 0$ Å, $x = +0.12$ Å. Within this approximation the vibrational expectation value for $\chi(x)$ takes the form

$$\langle|\chi|\rangle = \chi(0) + \chi_x \langle|x|\rangle + \frac{\chi_{xx}}{2} \langle|x^2|\rangle. \tag{24}$$

If the potential energy function, $V(x)$, would be symmetric, the vibrational ground state Ψ-function would be symmetric too with $\langle|x|\rangle = 0$ as the obvious consequence. However, $V(x)$ is anharmonic and the comparatively light deuterium atom probes this anharmonicity quite effectively. In the following we will demonstrate that the anharmonicity leads to first and second order contributions to $\langle|\chi(x)|\rangle$, which are similar in magnitude but opposite in sign and thus largely cancel.

Starting point of our consideration is the general rule, that the expectation value for the force, which acts on the vibrating atom, must vanish for all bound states. This is especially true for the ground state and may be written as

$$\left\langle \left| \frac{\mathrm{d}\, V(x)}{\mathrm{d}\, x} \right| \right\rangle = 0. \tag{25}$$

Now, for small x-values, the potential $V(x)$ may be expanded around its minimum at $x = 0$. With V_{xx} and V_{xxx} the second and third derivatives of $V(x)$ at the equilibrium position $x = 0$, we approximate this polynomial expansion as:

$$V(x) = \frac{V_{xx}}{2} x^2 + \frac{V_{xxx}}{6} x^3, \tag{26}$$

and the vibrational ground state expectation value (25), in which the Ψ-function only probes the immediate vicinity of $x = 0$, may be approximated as:

$$\left\langle \left| \frac{\mathrm{d}\, V(x)}{\mathrm{d}\, x} \right| \right\rangle = V_{xx} \langle|x|\rangle + \frac{V_{xxx}}{2} \langle|x^2|\rangle = 0 \tag{27}$$

or, rearranged:

$$\langle|x|\rangle = -\frac{V_{xxx}}{2V_{xx}} \langle|x^2|\rangle. \tag{28}$$

In the last step we approximate $\langle|x^2|\rangle$ by its value for the limiting harmonic oscillator:

$$\langle|x^2|\rangle = \frac{\hbar}{2\sqrt{V_{xx} m_{\mathrm{D}}}}. \tag{29}$$

This leads to

$$\langle|\chi(x)|\rangle = \chi(0) + \left[\chi_{xx} - \chi_x \frac{V_{xxx}}{V_{xx}}\right] \frac{\hbar}{4\sqrt{V_{xx} m_{\mathrm{D}}}}. \tag{30}$$

In our case the second and third derivatives of $V(x)$ follow from the Morse-potential as

$$V_{xx} = 2a^2 D \tag{31}$$

and

$$V_{xxx} = -6a^3 D \tag{32}$$

and the final expression for the expectation value of $\chi(x)$ takes the form

$$\langle|\chi(x)|\rangle = \chi(0) + [\chi_{xx} + 3a\chi_x] \frac{\hbar}{4\sqrt{2a^2 D m_D}}. \quad (33)$$

In Fig. 7 we present the functions $V(x)$ and $\chi(x)$ which follow from the MP2/6-31G(d,p) results at $x = 0$ Å and $x = \pm 0.12$ Å. Also shown is the corresponding vibrational ground state energy level and $|\Psi(x)|^2$ for the limiting harmonic oscillator, which was used to calculate the approximate value for $\langle|x^2|\rangle$. Note that a mere shift of probability density from a negative x-value to the corresponding positive x-value would leave $\langle|x^2|\rangle$ unchanged. Therefore the value of $\langle|x^2|\rangle$ responds comparatively slowly, if the anharmonicity is introduced. Because of the mutual compensation of the first and second order contributions, the χ-expectation value for the CD-stretching mode deviates comparatively little from the value calculated for the equilibrium configuration. It drops only on the order of one kHz for both molecules. This falls rather short with respect to the difference between the calculated ab initio value and our experimental values. However, a considerably larger correction is obtained for the bending mode, as we will show in the following section.

8.2.4. Bending Correction

Within our local mode picture described above, the Schrödinger equation for the "in-plane" CCD-bending motion takes the form

$$-\frac{\hbar^2}{2m_D r_{CD}^2}\frac{d^2\Psi(\varphi)}{d\varphi^2} + V(\varphi)\Psi(\varphi) = E\Psi(\varphi). \quad (34)$$

Here r_{CD} denotes the CD-bond distance for the equilibrium configuration.

From symmetry, the bending potential, $V(\varphi)$, and the quadrupole coupling "constant" in direction of the heavy atom chain, $\chi(\varphi)$, may be expanded into Taylor series which contain only even powers of φ . By inspection of the MP2/6-31G(d,p)-values for $V(\varphi)$ and $\chi(\varphi)$ for a grid of φ-values, we found that for bending angles below $\pm 40°$ already second order expansions lead to a satisfactory reproduction of the ab initio values for both molecules

$$V(\varphi) = \frac{V_{\varphi\varphi}}{2}\varphi^2 \quad (35)$$

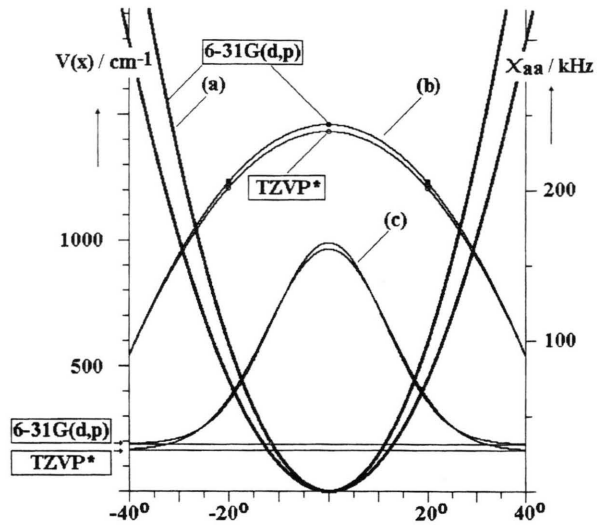

Fig. 8. MP2/6-31G(d,p) and MP2/TZVP* results for the pure CCD-bending vibration (see text). Traces a: φ-dependance of the potential $V(\varphi)$. Traces b: Variation of the deuterium coupling constant χ_{aa} in direction of the heavy atom chain with the bending angle φ. Traces c: Probability density $|\Psi(\varphi)|^2$. Also shown are the corresponding vibrational ground state energy levels.

and

$$\chi(\varphi) = \chi(0) + \frac{\chi_{\varphi\varphi}}{2}\varphi^2, \quad (36)$$

with the abbreviations

$$\chi_{\varphi\varphi} = \frac{\partial^2\chi(0)}{\partial\varphi^2} \quad (37)$$

and

$$V_{\varphi\varphi} = \frac{\partial^2 V(0)}{\partial\varphi^2}. \quad (38)$$

The parameters $V_{\varphi\varphi}$, $\chi(0)$, and $\chi_{\varphi\varphi}$ were fitted to the MP2-energies and χ-values at the equilibrium configuration and at a bending angle of $\varphi = 20°$. The corresponding plots are shown in Figure 8. We recall that within the harmonic approximation, the ground state wave function for the CCD-bending motion is given by

$$\Psi(\varphi) = \left(\frac{2\alpha}{\pi}\right)^{1/4} e^{-\alpha\cdot\varphi^2} \quad (39)$$

with

$$\alpha = \frac{\sqrt{V_{\varphi\varphi} m_D r_{CD}^2}}{2\hbar}. \tag{40}$$

The vibrational expectation value of χ then takes the approximate value

$$\langle|\chi(\varphi)|\rangle = \chi(0) + \frac{\chi_{\varphi\varphi}}{4} \frac{\hbar}{\sqrt{V_{\varphi\varphi} m_D r_{CD}^2}}. \tag{41}$$

For both molecules, insertion of the MP2/6-31G(d,p)-values for $\chi(0)$, $\chi_{\varphi\varphi}$, $V_{\varphi\varphi}$ and r_{CD} leads to a drop of χ by about 6 kHz as the result of this averaging over the in-plane bending motion. However, since the bending motion is two-fold degenerate, the complete CCD-bending correction for χ is twice as large, i.e. about 12 kHz in direction to lower values. Because of the additional bending motions, the overall bending correction must be even larger, which should shift the corrected ab initio values into even closer vicinity of the experimental values.

8.3.5. Basis Set Effects

The quality of the ab initio results for the quadrupole coupling constants clearly depends on the flexibility of the set of atomic basis functions which is used for the calculation. In order to get a quantitative impression of this dependence, we have used four sets of atomic basis functions:

1. The standard 6-31G(d,p) basis as included in the GAUSSIAN 94 program at all atoms.
2. The standard 6-31G(d,p) set of functions at the heavy atoms, C and F, and at H a considerably larger basis derived from Huzinagas work [48], as has been used by us earlier ([49], Table 12).
3. The basis set derived from Huzinagas work at H (see above) and a TZVP basis developed by Ahlrichs and coworkers [50] at C and F (see Table 13 in [49]).
4. The basis set derived from Huzinagas work at H and essentially the TZVP basis of Ahlrichs et al. but with decontracted p-orbitals and supplemented by two additional d-type orbitals at the heavy atoms with exponents $\zeta = 7.2$ and $\zeta = 0.8$ at C and $\zeta = 12.6$ and $\zeta = 1.4$ at F, respectively. This set is denoted as TZVP* in Figs. 8 and 9.

For all three extended basis sets we did run the MP2-routine as described before in order to get the corresponding energy relaxed equilibrium structures as well as the estimates for the vibrational corrections due to the deuterium CD-stretching and

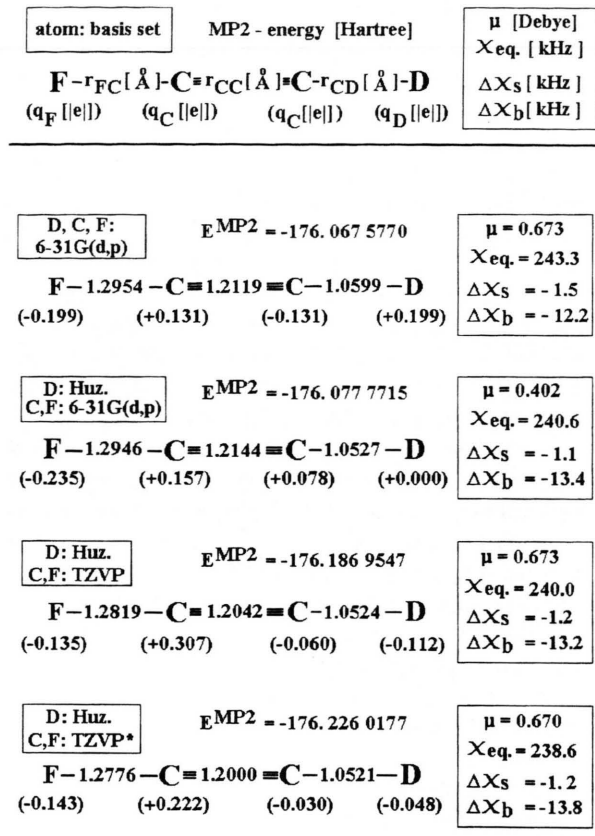

Fig. 9. FCCD: Basis set dependence of the energy relaxed bond distances, electric dipolemoment μ, deuterium quadrupole coupling constant χ, Mulliken charges q, and of the CD-streching and CCD-bending corrections to the χ values, which should be added to the equilibrium values: $\chi_{corr} = \chi_{eq} + \Delta\chi_s + \Delta\chi_b$. The experimental value of the dipolemoment is 0.73(3) D [28]. The experimental value for χ_{aa} is 210.9 ± 1.4 kHz. This work, Table 3.

CCD-bending modes. In Fig. 9 we present a synoptic view of these results for the monoacetylene, FCCD. The results for FCCCCD are almost identical as far as the values for the corrections are concerned.

From Fig. 9 it is seen that the MP2-values for χ drop systematically with each extension of the molecular basis set and thus come closer to the experimental values (compare Table 3). It may be also interesting to note that if a large basis set is provided only at the site of the quadrupole nucleus, as is in our second set, a shift of computed electron density towards the atom, equipped with the larger basis is the obvious result. The Mulliken atomic charges and the change in the electric dipole moment may

serve as indicators. This should be kept in mind, if only locally improved basis sets are used as a compromise between obtainable accuracy and computer time.

In conclusion we can state that the initial difference of 32.4 kHz between the MP2/6-31G(d,p) value for χ and its experimental value could be reduced to 12.7 kHz by using a larger set of atomic basis functions (reduction: 4.7 kHz), by roughly accounting for averaging over the CD-stretching χ mode (reduction: 1.2 kHz) and by roughly accounting for the averaging over the CCD-bending mode (reduction: 13.8 kHz). We therefore expect that a MP2-calculation with a molecular basis which at least corresponds to our fourth basis in quality and which properly accounts for all vibrational corrections (including anharmonicity) should be able to reproduce the experimental quadrupole coupling constants probably with kHz accuracy. Especially inclusion of the other bending vibrations should improve the calculated χ-values significantly.

8.3. General Remarks

It may be mentioned that the synthesis by discharge in a molecular beam provides a method to produce molecular species which are difficult and / or expensive to prepare. This confirms former results [1 - 5] and [10]. Together with the high sensitivity and resolution of MBFTMW spectroscopy it thereby provides the possibility to measure molecular constants with high precision, which would otherwise be difficult to determine.

Acknowledgement

We thank the members of the Kiel MW group, especially Dr. U. Andresen and Dr. J. Gripp, and Dr. J.-U. Grabow, TU Hannover, for help and discussion, Dr. G. Green, Kiel, for the advises to prepare the manuscript in Latex. Further we thank the mechanics and electronics workshop of the institute for indispensable help. The funds were provided by the Deutsche Forschungsgemeinschaft, the Fonds der Chemie and the Land Schleswig-Holstein.

[1] J.-U. Grabow, N. Heineking, and W. Stahl, Z. Naturforsch. **46a,** 914 (1991).
[2] C. Styger and M. C. L. Gerry, Chem. Phys. Lett. **188,** 213 (1992).
[3] C. Styger and M. C. L. Gerry, J. Mol. Spectrosc. **158,** 328 (1993).
[4] Y. Endo, H. Konguchi, and Y. Oshima, Faraday Discuss. **97,** 341 (1994) and subsequent publications.
[5] M. J. Travers, W. Chen, J.-U. Grabow, M. C. McCarthey, and P. Thaddeus, J. Mol. Spectrosc. **192,** 12 (1998) and subsequent publications.
[6] H. Dreizler, Ber. Bunsenges. Phys. Chem. **99,** 1451 (1995).
[7] M. D. Harmony, K. A. Beran, D. M. Angst, and K. L. Ratzlaff, Rev. Sci. Instrum. **66,** 5196 (1995).
[8] N. Hansen, H. Mäder, and F. Temps, Chem. Phys. Lett. **327,** 97 (2000).
[9] N. Hansen, Dissertation, Universität Kiel 2000.
[10] D. H. Sutter and H. Dreizler, Z. Naturforsch. **55a,** 695 (2000).
[11] A. E. Laird and J. K. Tyler, C. S. Chem. Comm. **1978,** 335.
[12] S. R. Lin and Y. P. Lee, J. Chem. Phys. **111,** 9233 (1999).
[13] J. U. Grabow, Dissertation, Universität Kiel (1992), Chapt. IV.
[14] O. Böttcher and D. H. Sutter, Z. Naturforsch. **43a,** 47 (1988).
[15] I. Merke and H. Dreizler, Z. Naturforsch. **43a,** 196 (1988).
[16] J. Haekel and H. Mäder, Z. Naturforsch. **43a,** 203 (1988).
[17] H. Jones and H. D. Rudolph, Z. Naturforsch. **34a,** 340 (1979).
[18] A. Guarnieri, private communication, 1999.
[19] J. K. Holland, D. A. Newnham. I. Mills, and H. Herman, J. Mol. Spectrosc. **151,** 346 (1992).
[20] W. Gordy and R. L. Cook, Microwave Molecular Spectra, J. Wiley, New York 1984, Chapt. V,1, p. 131.
[21] V. W. Weiss, H. D. Todd, Mei-Kuo Lo, H. S. Guttowsky, and W. H. Flygare, J. Chem. Phys. **47,** 4021 (1967).
[22] W. H. Flygare, Molecular Structure and Dynamics, Prentic-Hall, Englewoods Cliffs, New Jersey 1978, Chapt. 6.9, Eq. (6-131, 6-133).
[23] W. Gordy and R. L. Cook, Microwave Molecular Spectra, J. Wiley, New York 1984, Chapt. IX,7, XV,1.
[24] W. Gordy and R. L. Cook, Microwave Molecular Spectra, J. Wiley, New York 1984, Chapt. XV,5.
[25] W. Gordy and R. L. Cook, Microwave Molecular Spectra, J. Wiley, New York 1984, Appendix E.
[26] Programs QSSR.FOR and QSSRFIT.FOR written by G. L. Blackman, B. Kleibömer, W. Stahl, and N. Heineking.
[27] W. Gordy and R. L. Cook, Microwave Molecular Spectra, J. Wiley, New York 1984, Chapt. XV,1.

[28] T. K. Tyler and J. Sheridan, Trans Faraday Soc. **59,** 2661 (1963).
[29] V. W. Weiss and W. H. Flygare, J. Chem. Phys. **45,** 8 (1966).
[30] N. Heineking, M. Andolfatto, C. Kruse, W. Eberstein, and H. Dreizler, Z. Naturforsch. **43a,** 755 (1988).
[31] W. Hüttner, H. K. Bodenseh, and P. Novicki, Mol.Phys. **35,** 729 (1978).
[32] K. Matsumura, K. Tanaka, and C. Yamada, J. Mol. Spectrosc. **80,** 209 (1980).
[33] W. Gordy and R. L. Cook, Microwave Molecular Spectra, J. Wiley, New York 1984, Chapt. IX,4.
[34] C. H. Townes and A. L. Schawlow, Microwave Spectroscopy, McGraw Hill Book Co. Inc., New York 1955, Chapt. 6.
[35] T. Okabayashi, K. Tanaka, and T. Tanaka, J. Mol. Spectrosc. **137,** 9 (1989).
[36] L. Dore, L. Cludi, A. Mazzavillani, G. Cazzoli, and C. Puzzarini, Phys. Chem. Chem. Phys. **1,** 2275 (1999).
[37] C. H. Townes and A. L. Schawlow, Microwave Spectroscopy, McGraw Hill Book Co. Inc., New York 1955, Chapt. 8.7 - 8.9.
[38] W. Gordy and R. L. Cook, Microwave Molecular Spectra, J. Wiley, New York 1984, Chapt. IX,7.
[39] F. DeLucia and W. Gordy, Phys. Rev. **187,** 58 (1969), Eq. (16).
[40] D. A. Jennings and J. S. Wells, J. Mol. Spectrosc. **130,** 267 (1988).
[41] F. DeLucia and W. Gordy, Phys. Rev. A **3,** 1849 (1971).
[42] J. S. Muenter and W. Klemperer, J. Chem. Phys. **52,** 6033 (1970).
[43] H. Huber, J. Chem. Phys. **83,** 4591 (1985).
[44] H. Huber and P. Diehl, Mol. Phys. **54,** 725 (1985).
[45] S. Gerber and H. Huber, J. Mol. Spectosc. **134,** 168 (1989).
[46] Gaussian 94, Revision C.3, M. J. Frisch, G. W. Trucks, H. B. Schlegel, P. M. W. Gill, B. G. Johnson, M. A. Robb, J. R. Cheeseman, T. Keith, G. A. Petterson, J. A. Montgomery, K. Raghavachari, M. A. Al-Laham, V. G. Zakrzewski, J. V. Ortiz, J. B. Foresman, J. Cioslowski, B. B. Stefanov, A. Nanayakkara, M. Challacombe, C. Y. Peng, P. Y. Ayala, W. Chen, M. W. Wong, J. L. Andres, E. S. Replogle, R. Gomperts, R. L. Martin, D. J. Fox, J. S. Binkley, D. J. Defrees, J. Baker, J. P. Stewart, M. Head-Gordon, C. Gonzalez, and J. A. Pople, Gaussian, Inc., Pittsburgh (Pa) 1995.
[47] C. Møller and M. S. Plesset, Phys. Rev. **46,** 618 (1934).
[48] S. Huzinaga, J. Chem. Phys. **42,** 1293 (1965), Table V.
[49] S. Antonilez, J. L. Alonso, H. Dreizler, E. Hentrop, and D. H. Sutter, Z. Naturforsch. **54a,** 524 (1999).
[50] A. Schäfer, H. Horn, and R. Ahlrichs, J. Chem. Phys. **97,** 2571 (1992).